united nations
educational, scientific
and cultural
organization

international atomic
energy agency

the
abdus salam
international centre for theoretical physics

ICTP 40th Anniversary

H4.SMR/1574-15

"VII School on Non-Accelerator Astroparticle Physics"

26 July - 6 August 2004

Neutrino Masses and Mixing - II

S. Petcov

SISSA/INFN, Trieste, Italy &
INRNE, Bulgarian Academy of Sciences, Sofia
Bulgaria

Experiments with $\nu_\odot$:

- Davis et al. '67-'98 (Cl-Ar; ^8B, ^7Be,)
- Kamiokande II, III ($\nu + e^-$; ^8B) '86-'94
- SAGE '90- (Ga-Ge; pp, ^7Be, ^8B)
- GALLEX/GNO '91-

sensitive to $\Delta m^2 \gtrsim 10^{-11}\ eV^2$

- SUPER-KAMIOKANDE (SK) ($\nu + e^-$; ^8B) '96-
- SNO '99- ($\nu_e + D \to e^- + p + p$ CC
  $\nu + D \to \nu + p + n$ NC
  $\nu + e^- \to \nu + e^-$ ES
  ^8B)

NATIONAL RESEARCH COUNCIL OF CANADA

DIVISION OF ATOMIC ENERGY

INVERSE β PROCESS

by

B. Pontecorvo

Chalk River, Ontario

20 November, 1946

PD-205

A bit of History $\nu_\odot$

1946 : B. Pontecorvo (Chalk River Lab. Report № PD 205)

Reactors - copious sources of neutrinos.
The Sun

Flux estimations :

detection of (reactor / solar) neutrinos (feasible / difficult but possible)

(Flux of $\nu_\odot$ at the Earth surface:

B.P. $10^{10} \frac{\nu_e}{cm^2\ sec}$;

today $6.5.10^{10} \frac{\nu_e}{cm^2\ sec}$.)

The radiochemical Cl - Ar method of ν detection was also suggested. (Discussed by ALVAREZ in 1949)

1954 - 1956 Reines + Cowen

1955 - ... R. Davis.

A brief summary of the data and the relevant SSM predictions

$\nu_\odot$ - flux:

Component	PP	^{7}Be	^{8}B	pep	^{13}N	^{15}O
E_{max} (MeV)	0.42	0.86; 0.38	14	1.44	1.2	1.73
$\bar{E}$ (MeV)	0.26	0.86; 0.38	6.7	1.44	0.71	1.0

Rep 18 MeV?

Method of $\nu_\odot$-Detection

	Cl - Ar	$\nu + e^- \rightarrow \nu + e^-$	
Collab.	Davis et al.	K - II, K - III,	S-K
E_{th} [MeV]	0.81	7.5	7.0 / 6.5 / 5.0
$\nu_\odot$-flux comp.	^{8}B, ^{7}Be, other, PP	^{8}B	
Contribution (%)	70÷77, 17÷14, 13÷9, 0.0	100	
(SSM - all authors)	66÷, 22÷		
Dar, Shaviv!			

	Ga - Ge
	SAGE, GALLEX/GNO
	0.233
	^{8}B, ^{7}Be, PP, other
Contribution (%)	10÷7.4 ÷6; 27÷24; 54÷57 ÷60; 9÷12 8÷

The Status of the Solar Neutrino Problem

Neutrinos are produced in the Sun in the following reactions:

$$p + p \rightarrow D + e^+ + \nu_e \quad (99.75\%)$$

$E_\nu \leq 0.42$ MeV, $\bar{E}_\nu = 0.26$ MeV

$$p + p + e^- \rightarrow D + \nu_e \quad (0.25\%)$$

$E_\nu = 1.44$ MeV

SSM: (98.5%) of the energy released in the Sun is produced in the chain of reactions beginning with these two

$$^7_4Be + e^- \rightarrow ^7_3Li + \nu_e \qquad (^3_2He + ^4_2He \rightarrow ^7_4Be + \gamma)$$

$E_\nu = \begin{cases} 0.86 \text{ MeV} & (90\%) \\ 0.38 \text{ MeV} & (10\%) \end{cases}$

$$^8_5B \rightarrow ^8_4Be^* + e^+ + \nu_e \qquad (^7_4Be + p \rightarrow ^8_5B + \gamma)$$

$E_\nu \leq 14$ MeV, $\bar{E}_\nu = 7.2$ Me

$$^{13}_7N \rightarrow ^{13}_6C + e^+ + \nu_e$$

$E_\nu \leq 1.2$ MeV, $\bar{E}_\nu \cong 0.71$ MeV

$$^{15}_8O \rightarrow ^{15}_7N + e^+ + \nu_e$$

$E_\nu \leq 1.73$ MeV, $\bar{E}_\nu \cong 1$ MeV

(CNO - chain)

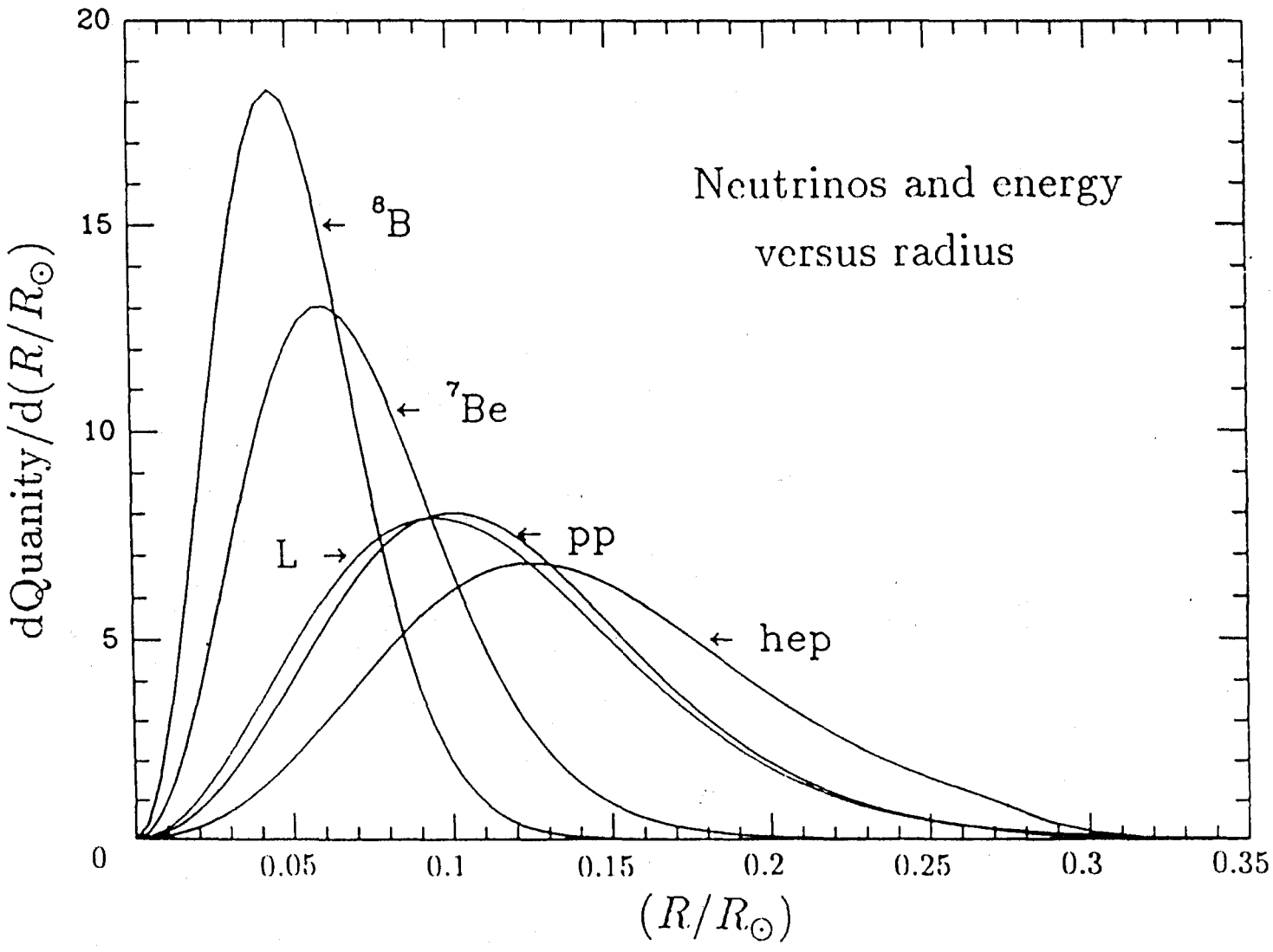
Neutrinos and energy
versus radius
dQuanity/d$(R/R_\odot)$
$(R/R_\odot)$
^{8}B
^{7}Be
pp
hep
L
0
5
10
15
20
0.05
0.1
0.15
0.2
0.25
0.3
0.35

Table 1: Nuclear reactions in the Sun (pp-chain)

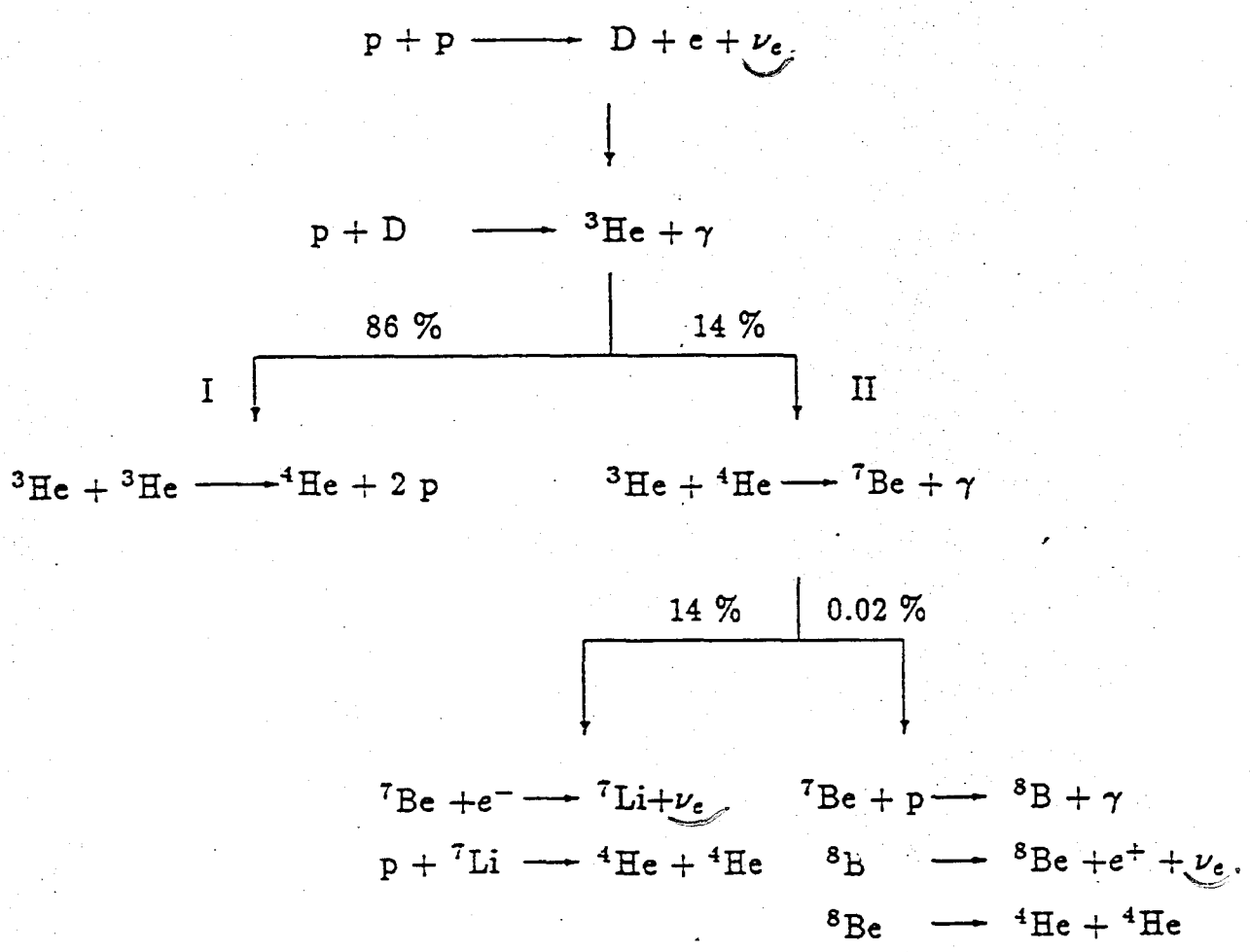

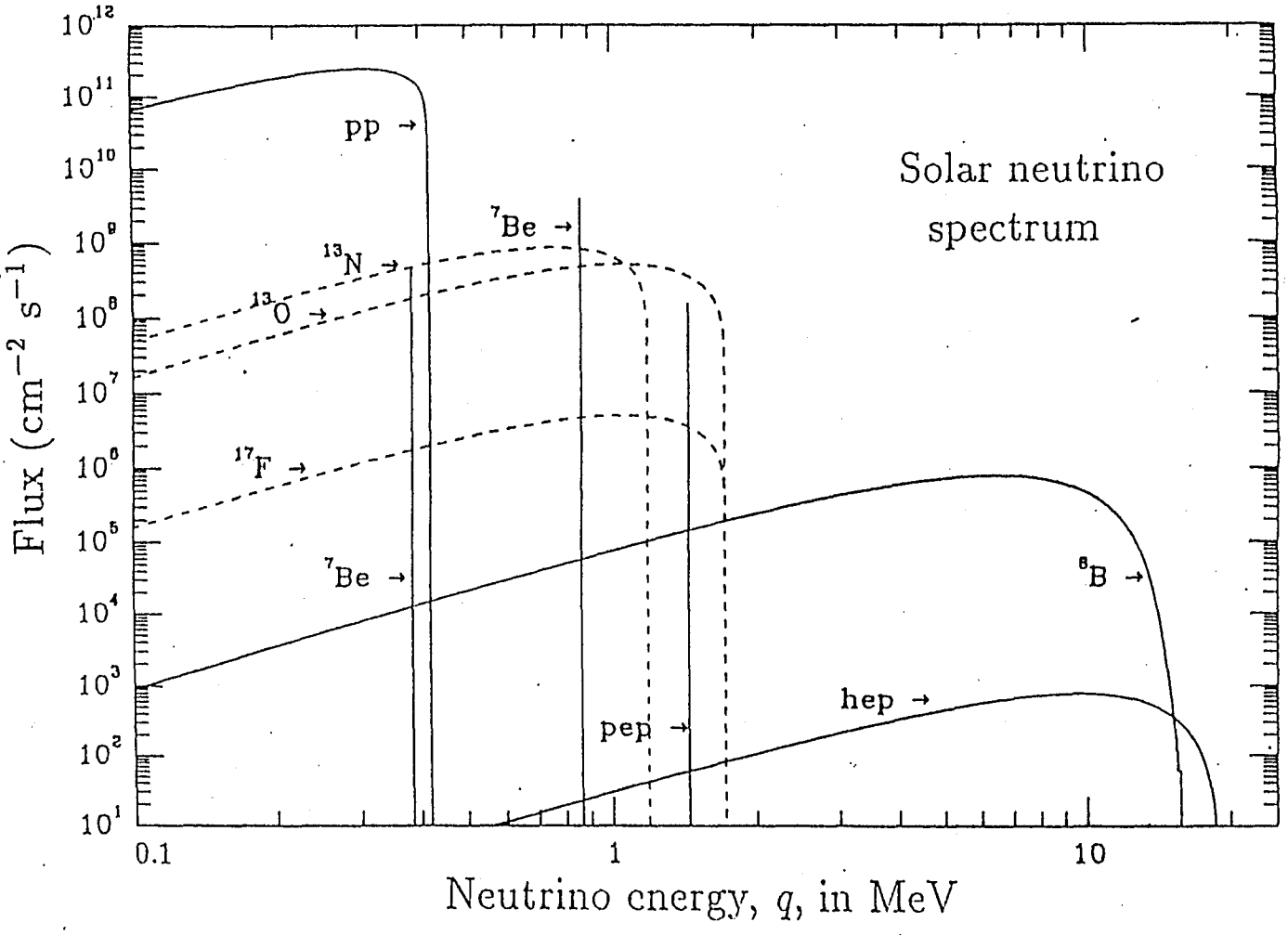

Figure 6.4 Solar neutrino spectrum This figure shows the energy spectrum of neutrinos that is predicted by the standard solar model discussed in Section 4.3. The neutrino fluxes from continuum sources are given in the units of number per cm^2 per second per MeV at one astronomical unit and the line fluxes are given in number per cm^2 per second. The spectra from the pp chain are drawn with solid lines; the CNO spectra are drawn with dotted lines.

What Do We (Not) Know Theoretically about Solar Neutrino Fluxes?

John N. Bahcall*
School of Natural Sciences, Institute for Advanced Study, Princeton, New Jersey 08540, USA
M. H. Pinsonneault†
Department of Astronomy, The Ohio State University, Columbus, Ohio 43210, USA
(Received 16 December 2003; published 25 March 2004)

Solar model predictions of ^{8}B and p-p neutrinos agree with the experimentally determined fluxes (including oscillations): $\phi(pp)_{\text{measured}} = (1.02 \pm 00.02 \pm 0.01)\phi(pp)_{\text{theory}}$ and $\phi(^8\text{B})_{\text{measured}} = (0.88 \pm 0.04 \pm 0.23)\phi(^8\text{B})_{\text{theory}}$, 1σ experimental and theoretical uncertainties, respectively. We use improved input data for nuclear fusion reactions, the equation of state, and the chemical composition of the Sun. The solar composition is the dominant uncertainty in calculating the ^{8}B and CNO neutrino fluxes; the cross section for the ^{3}He(^{4}He, γ)^{7}Be reaction is the most important uncertainty for the calculated ^{7}Be neutrino flux.

DOI: 10.1103/PhysRevLett.92.121301 PACS numbers: 26.65.+t, 14.60.Pq, 96.60.Jw

This Letter is part of a series that spans more than 40 years [1]. The goals of this series are to provide increasingly more precise theoretical calculations of the solar neutrino fluxes and detection rates and to make increasingly more comprehensive evaluations of the uncertainties in the predictions. We describe here two steps forward (improved accuracy of the equation of state of the solar interior and some of the nuclear fusion data) and one step backward (increased systematic uncertainties in the determination of the surface composition of the Sun).

Using recent improvements in input data, we calculate the best estimates, and especially the uncertainties, in the solar model predictions of solar neutrino fluxes. We compare the calculated neutrino fluxes with their measured values. We stress the need for more accurate measurements of the surface composition of the Sun and of specific nuclear reaction rates.

Table I presents, in the second (third) column, labeled BP04 (BP04+), our best solar model calculations for the neutrino fluxes. The uncertainties are given in column 2. BP04+ was calculated with new input data for the equation of state [4], nuclear physics [5,6], and solar composition [7]. BP04, our currently preferred model, is the same as BP04+ except that BP04 does not include the most recent analyses of the solar surface composition [7], which conflict with helioseismological measurements. The error estimates, which are the same for BP04, BP04 +, and ^{14}N (see Table I), include the recent composition analyses.

For the BP04 solar model, the base (mass) of the convective zone is $0.715R_\odot$ ($0.024M_\odot$), the surface heavy element to hydrogen ratio by mass, $Z/X = 0.0229$, the surface helium abundance is 0.243, and 1.6% of the luminosity is from CNO reactions. The central temperature, helium abundance, and Z/X are, respectively, 15.72×10^6 K, 0.640, and 0.0583. All of these values are in the acceptable range as determined by helioseismology. However, for BP04+, the base of the convective zone (CZ) is $R_{\text{CZ}}/R_\odot = 0.726$, which conflicts with the measured value of 0.713 ± 0.001 (or ± 0.003; see Ref. [8]). By examining a series of models, we have determined that the reason for the too-shallow CZ in the BP04+ model is the lower heavy element abundance, $Z/X = 0.0176$. Therefore, we prefer BP04.

The measurements from different solar neutrino experiments [9] and the KamLAND reactor data [10] can be combined in a global analysis to obtain the best empirical values for the p-p, ^{8}B, and ^{7}Be solar neutrino fluxes. We use the fluxes from the global analysis of Ref. [11], which allows all the solar neutrino fluxes to be free parameters subject only to the luminosity constraint (i.e., energy conservation). Comparing the measured values with the theoretical predictions, we find for BP04:

$$\phi(pp)_{\text{measured}} = (1.02 \pm 0.02 \pm 0.01)\phi(pp)_{\text{theory}}, \quad (1)$$

$$\phi(^8\text{B})_{\text{measured}} = (0.88 \pm 0.04 \pm 0.23)\phi(^8\text{B})_{\text{theory}}, \quad (2)$$

$$\phi(^7\text{Be})_{\text{measured}} = (0.91^{+0.24}_{-0.62} \pm 0.11)\phi(^7\text{Be})_{\text{theory}}. \quad (3)$$

In Eqs. (1)–(3), the 1σ experimental uncertainties are given before the 1σ theoretical uncertainties.

The measured and theoretical values for the fluxes agree within their combined 1σ uncertainties. The measurement error of the ^{8}B neutrino flux is smaller than the uncertainty in the theoretical calculation; but the opposite is true for the p-p and ^{7}Be neutrino fluxes.

Column 4 of Table I presents the fluxes calculated using our previous best solar model, BP00 [2]. The BP04 best estimate neutrino fluxes and their uncertainties have not changed markedly from their BP00 values despite refinements in input parameters. The only exception is the CNO flux uncertainties that have almost doubled due to the larger systematic uncertainty in the surface chemical composition estimated in this Letter.

We describe improvements in the input data relative to BP00. Quantities that are not discussed here are the same

TABLE I. Predicted solar neutrino fluxes from solar models. The table presents the predicted fluxes, in units of $10^{10}(pp)$, $10^{9}(^{7}\mathrm{Be})$, $10^{8}(pep, {}^{13}\mathrm{N}, {}^{15}\mathrm{O})$, $10^{6}(^{8}\mathrm{B}, {}^{17}\mathrm{F})$, and $10^{3}(hep)$ $\mathrm{cm}^{-2}\,\mathrm{s}^{-1}$. Columns 2–4 show BP04, BP04 +, and our previous best model BP00 [2]. Columns 5–7 present the calculated fluxes for solar models that differ from BP00 by an improvement in one set of input data: nuclear fusion cross sections (column 5), equation of state for the solar interior (column 6), and surface chemical composition for the Sun (column 7). Column 8 uses the same input data as for BP04 except for a recent report of the $^{14}\mathrm{N} + p$ fusion cross section. References to the improved input data are given in the text. We use OPAL radiative opacities calculated for each chemical composition. The last two rows ignore neutrino oscillations and present for the chlorine and gallium solar neutrino experiments the capture rates in SNU (1 SNU equals 10^{-36} events per target atom per sec). Because of oscillations, the measured rates are smaller: 2.6 ± 0.2 and 69 ± 4, respectively. We use the neutrino absorption cross sections and their uncertainties that are given in Ref. [3].

Source	BP04	BP04+	BP00	Nucl.	EOS	Comp.	^{14}N
pp	$5.94(1 \pm 0.01)$	5.99	5.95	5.94	5.95	6.00	5.98
pep	$1.40(1 \pm 0.02)$	1.42	1.40	1.40	1.40	1.42	1.42
hep	$7.88(1 \pm 0.16)$	8.04	9.24	7.88	9.23	9.44	7.93
^{7}Be	$4.86(1 \pm 0.12)$	4.65	4.77	4.84	4.79	4.56	4.86
^{8}B	$5.79(1 \pm 0.23)$	5.26	5.05	5.77	5.08	4.62	5.74
^{13}N	$5.71(1^{+0.37}_{-0.35})$	4.06	5.48	5.69	5.51	3.88	3.23
^{15}O	$5.03(1^{+0.43}_{-0.39})$	3.54	4.80	5.01	4.82	3.36	2.54
^{17}F	$5.91(1^{+0.44}_{-0.44})$	3.97	5.63	5.88	5.66	3.77	5.85
Cl	$8.5^{+1.8}_{-1.8}$	7.7	7.6	8.5	7.6	6.9	8.2
Ga	131^{+12}_{-10}	126	128	130	129	123	127

as for BP00. Each class of improvement is represented by a separate column, columns 5–7, in Table I.

Column 5 contains the fluxes computed for a solar model that is identical to BP00 except that we have used improved values for direct measurements of the $^{7}\mathrm{Be}(p, \gamma)^{8}\mathrm{B}$ cross section, $S_{20\,\mathrm{keV}}(^{7}\mathrm{Be} + p) = 20.6 \pm 0.8$ eV b [5], and the calculated *p-p*, $S_0(pp) = 3.94(1 \pm 0.004) \times 10^{-25}$ MeV b, and *hep*, $S_0(hep) = (8.6 \pm 1.3) \times 10^{-20}$ keV b, cross sections [6]. The reactions that produce the ^{8}B and *hep* neutrinos are rare; changes in their production cross sections affect, respectively, only the ^{8}B and *hep* fluxes. The 15% increase in the calculated ^{8}B neutrino flux, which is primarily due to a more accurate cross section for $^{7}\mathrm{Be}(p, \gamma)^{8}\mathrm{B}$, is the only significant change in the best estimate fluxes.

The fluxes in column 6 were calculated using a refined equation of state [4]. Solar neutrino calculations are insensitive to the present level of uncertainties in the equation of state.

The most important changes in the astronomical data since BP00 result from new analyses of the surface chemical composition of the Sun. The input chemical composition affects the radiative opacity and hence the physical characteristics of the solar model, as well as, to a lesser extent, the nuclear reaction rates. New values for C, N, O, Ne, and Ar have been derived [7] using three-dimensional rather than one-dimensional atmospheric models, including hydrodynamical effects, and paying particular attention to uncertainties in atomic data and observational spectra. The new abundance estimates, together with the previous best estimates for other solar surface abundances [12], imply $Z/X = 0.0176$, much less than the previous value of $Z/X = 0.0229$ [12]. Column 7 gives the fluxes calculated for this new composition mixture. The largest change in the neutrino fluxes for the *p-p* chain is the 9% decrease in the predicted ^{8}B neutrino flux. The N and O fluxes are decreased by much more, ~35%, because they reflect directly the inferred C and O abundances.

The CNO nuclear reaction rates are less well determined than the rates for the more important (in the Sun) *p-p* reactions [13]. The rate for $^{14}\mathrm{N}(p, \gamma)^{15}\mathrm{O}$ is poorly known, but important for calculating CNO neutrino fluxes. Extrapolating to the low energies relevant for solar fusion introduces a large uncertainty. Column 8 gives the neutrino fluxes calculated with input data identical to BP04 except for the cross section factor $S_0(^{14}\mathrm{N} + p) = 1.77 \pm 0.2$ keV b that is about half the current best estimate; this value assumes a particular *R*-matrix fit to the experimental data [14]. The *p-p* cycle fluxes are changed by only ~1%, but the ^{13}N and ^{15}O neutrino fluxes are reduced by 40%–50% relative to the BP04 predictions. CNO nuclear reactions contribute 1.6% of the solar luminosity in the BP04 model and only 0.8% in the model with a reduced $S_0(^{14}\mathrm{N} + p)$.

Table II shows the individual contributions to the flux uncertainties. Columns 2–5 present the fractional uncertainties from the nuclear reactions whose measurement errors are most important for calculating neutrino fluxes. Unless stated otherwise, we have used throughout this Letter the uncertainties estimated in Ref. [13] for nuclear cross sections.

The measured rate of the $^{3}\mathrm{He}$-$^{3}\mathrm{He}$ reaction, which after the inception of this series [1] changed by a factor of 4, and the measured rate of the $^{7}\mathrm{Be} + p$ reaction, which for most of this series has been the dominant uncertainty in

THE EXPERIMENTAL RESULTS

Cl-Ar [SNU]
(DAVIS et al., 1971-1996)

APRIL '37 : $2.56 \pm 0.16 \pm 0.14$
~ 800eV

$\nu + e^- \to \nu + e^-$ [10^6 ν/cm^2/sec]

KII + KIII

$2.80 \pm 0.19 \pm 0.33$ (± 0.38)
June '96, ~ 600eV

SUPER K

374 d, ~4950 eV
$2.37 \pm 0.06 \pm 0.09$ $-0.05 - 0.07$
$(+0.11/-0.09)$

540 d, ~ 6823 eV
$2.44 \pm 0.05 \pm 0.09$ $- 0.07$
825 d, ~ 11200 eV
$2.45 \pm 0.04 \pm 0.07$

1496 d, ~22400 eV
$2.35 \pm 0.02 \pm 0.08$
STAT

Ga-Ge [SNU]

GALLEX

65 runs, 300

$76.4 \pm 6.3 \pm 4.5$ -4.9

Final: 77.5 ± 6.2 ± 4.3 ± 4.7

SAGE

33 runs, ~100eV
Sept. '97
$73 \pm 8.5 \pm 5.2$ -6.9

'98:
$66.6 \pm 6.8 \pm 3.8$ $-7.1 - 4.0$

'02:
$70.9 \pm 5.3 \pm 3.7$ $-5.2 - 3.2$

'04:
$66.9 \pm 3.9 \pm 3.$

GALLEX/GNO

'02: $70.8 \pm 4.5 \pm 3.$

'04: $69.3 \pm 4.1 \pm 3.$

THE PREDICTIONS:

	Cl-Ar	$\nu + e^- \to \nu + e^-$	Ga-Ge
BP '00	7.5 ± 1.0	$(5.15 \pm 1.0 - 0.7) \times 10^6$	128 ± 8

J. BAHCALL, M.C. GONZALEZ-GARCIA
C. PEÑA-GARAY, '04

Experiment	Observable (# Data)	Measured/SM	Reference
Chlorine	Average Rate (1)	[CC]=0.30 ± 0.03	[8]
SAGE+GALLEX/GNO†	Average Rate (1)	[CC]=0.52 ± 0.03	[3, 4, 5]
Super-Kamiokande	Zenith Spectrum (44)	[ES]=0.406 ± 0.013	[10]
SNO (pure D_2O phase)	Day-night Spectrum (34)	[CC]=0.31 ± 0.02	[13, 14]
		[ES]=0.47 ± 0.05	[13, 14]
		[NC]=1.01 ± 0.13	[13, 14]
SNO (salt phase)	Average Rates (3)	[CC]=0.28 ± 0.02	[12]
		[ES]=0.38 ± 0.05	[12]
		[NC]=0.90 ± 0.08	[12]
KamLAND	Spectrum (10)	[CC]=0.69 ± 0.06	[6]
CHOOZ	Spectrum (14)	[CC] = 1.01 ± 0.04	[7]
K2K	Spectrum (6)	[CC]$(\nu_\mu) = 0.70^{+0.11}_{-0.10}$	[29]
Atmospheric	Zenith Angle Distributions (55)	[0.5-1.0]	[30]

† SAGE rate: $66.9 \pm 3.9 \pm 3.6$ SNU [3]; GALLEX/GNO rate: $69.3 \pm 4.1 \pm 3.6$ SNU [4, 5].

Table 1: Experimental data. We summarize the solar, reactor, accelerator, and atmospheric data used in our global analyses. Only experimental errors are included in the column labelled Result/SM. Here the notation SM corresponds to predictions of the Bahcall-Pinsonneault standard solar model (BP04) of ref. [31] and the standard model of electroweak interactions [32] (with no neutrino oscillations). The new average gallium rate is 68.1 ± 3.75 SNU (see ref. [2]). The SNO rates (pure D_2O phase) in the column labelled Result/SM are obtained from the published SNO spectral data by assuming that the shape of the ^{8}B neutrino spectrum is not affected by physics beyond the standard electroweak model. However, in our global analyses, we allow for spectral distortion. The SNO rates (salt phase) are not constrained to the ^{8}B shape [12]. The K2K and atmospheric data are used only in the analysis of θ_{13}, which is discussed in Appendix A.

Methods of $\nu_\odot$ Detection.

B. Pontecorvo: (1946)

$$\nu_e + {}^{37}Cl \rightarrow e^- + {}^{37}Ar$$

($T_{1/2} \approx 35$ days: ${}^{37}Ar + e^- \rightarrow {}^{37}Cl^* + \nu_e$)

$E_{th} = 0.81$ MeV $\Rightarrow$ (${}^8B$, ${}^7Be$ ν's) 2,8k

V. Kuzmin: (1965)

$$\nu_e + {}^{71}Ga \rightarrow e^- + {}^{71}Ge$$

($T_{1/2} \approx 11.4$ days)

$E_{th} = 0.233$ MeV $\Rightarrow$ (pp, ${}^7Be$ (${}^8B$))

"Recently": (1987...)

$$\nu + e^- \rightarrow \nu + e^-$$

$E_{th} \approx (8-9)$ MeV $\Rightarrow$ (${}^8B$)

7.5 MeV

R. Davis et al. **1970 - 1996 ...**

615 tons of C_2Cl_4 (in a gold mine in South Dakota at a depth of 4400 m of w.e. ~ 1500 m)

^{37}Ar: extracted and detected by using radiochemical methods.

Extraction : after (35-50) days of exposure

The observed average rate of ^{37}Ar production is **0.47 ± 0.04 ^{37}Ar atoms/day**

(Background: (0.08 ± 0.03) ^{37}Ar atoms/day)

The Results :

1970 - 1985	1986 - 1988
$(2,1 \pm 0.3)$ SNU	→ (4.2 ± 0.7) SNU
	(5.0 ± 1.0) SNU
	(3.6 ± 0.7) SNU

(* Munich, '88; ** Nof Ginozar, '89)

$$1\,SNU \equiv 10^{-36} \frac{\nu_\odot \text{ captures}}{\text{sec} \cdot \text{target atom}}$$

^{37}Cl ; ^{71}Ga, ...

The SSM prediction : **$(7,9 \pm 2.6)$ SNU**

(J. Bahcall, R. Ulrich, 1988)

effective 3σ error

R. Davis et al.,
1970 - 1989 **(2.33 ± 0.25) SNU**

("Inside the Sun", '89,)
Prog. p. 131

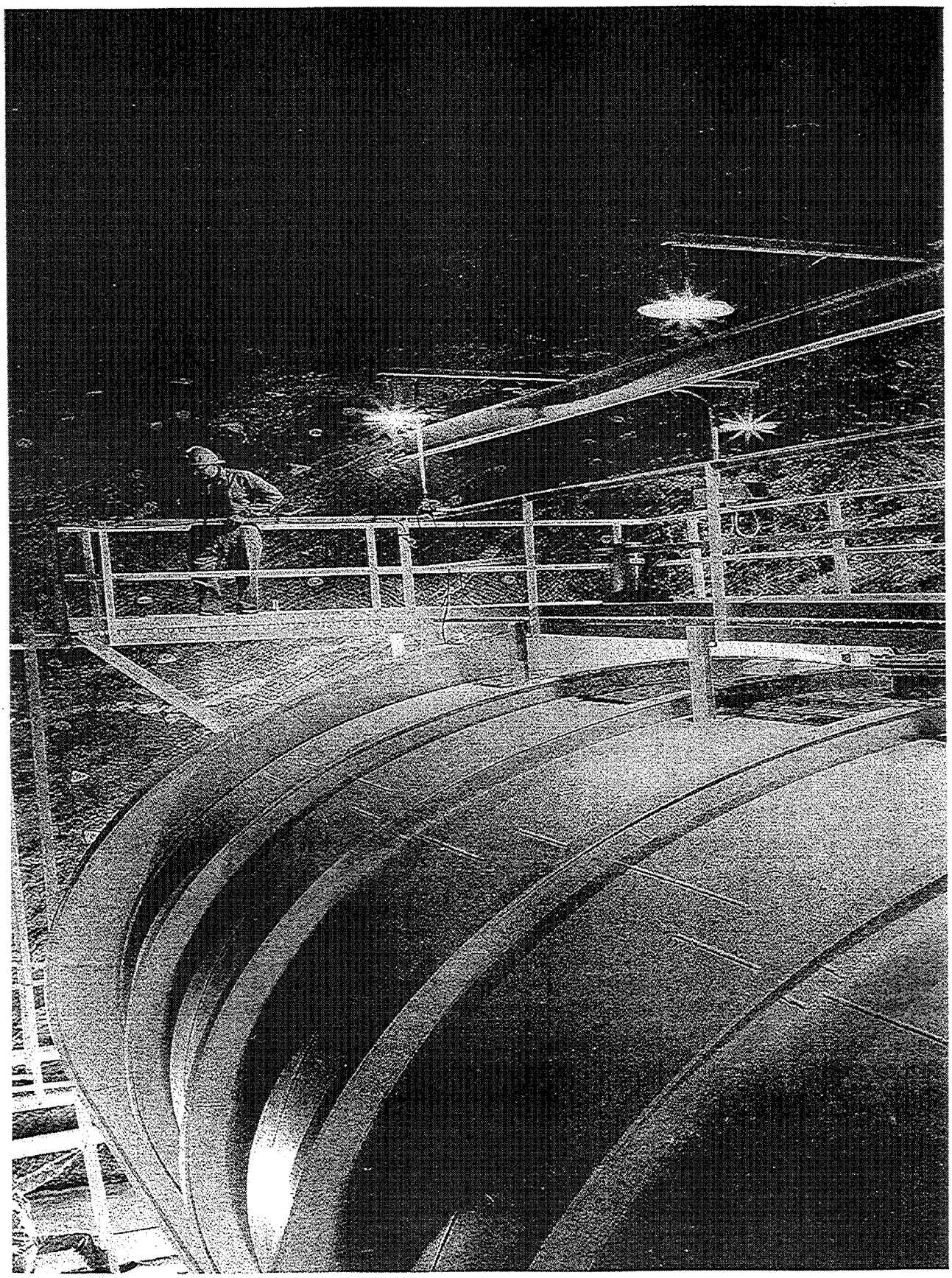

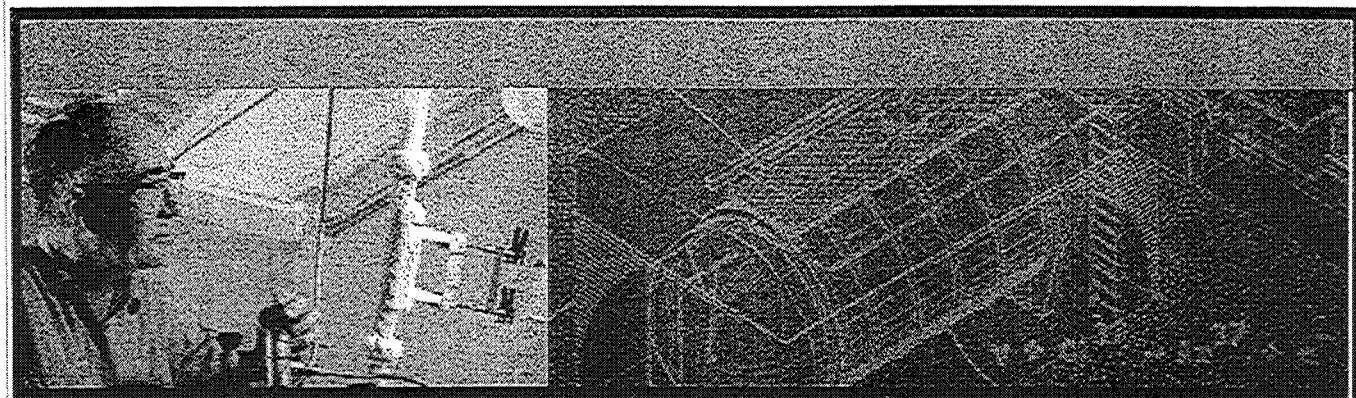

Raymond Davis Jr.

Raymond Davis Jr. earned a 1937 B.S. and 1940 M.S. from the University of Maryland, and a Ph.D. in physical chemistry from Yale University, 1942. After his 1942-46 service in the U.S. Army Air Force and two years with the Monsanto Chemical Company, he came to **Brookhaven National Laboratory** in 1948 to join the staff of the Chemistry Department. He received tenure in 1956 and was named senior chemist in 1964. Retiring from the Laboratory in 1984, Davis joined the University of Pennsylvania in 1985, but maintains an active appointment at Brookhaven as a research collaborator in the Chemistry Department.

A member of the National Academy of Sciences and the American Academy of Arts and Sciences, Davis has won numerous scientific awards, including the 1978 Cyrus B. Comstock Prize from the National Academy of Sciences; the 1988 Tom W. Bonner Prize from the American Physical Society; the 1992 W.K.H. Panofsky Prize, also from APS; the 1999 Bruno Pontecorvo Prize from the Joint Institute for Nuclear Research in Dubna, Russia; the 2000 Wolf Prize in Physics, which he shared with Masatoshi Koshiba, University of Tokyo, Japan; the **2002 National Medal of Science**; and the **Nobel Prize in Physics** in 2002 (shared with Masatoshi Koshiba of Japan, and Riccardo Giacconi of the U.S).

From 1971-73, he was a member of the National Aeronautics & Space Administration's Lunar Sample Review Board, and was involved in the analysis of lunar dust and rocks collected by the crew of Apollo 11 on NASA's historic first flight to the moon.

Davis was born in Washington, D.C., on October 14, 1914. He and his wife Anna are residents of Blue Point, New York. They have five grown children.

Research | **Images** | **Publications** | **Reminiscences** | **Brookhaven Lab**

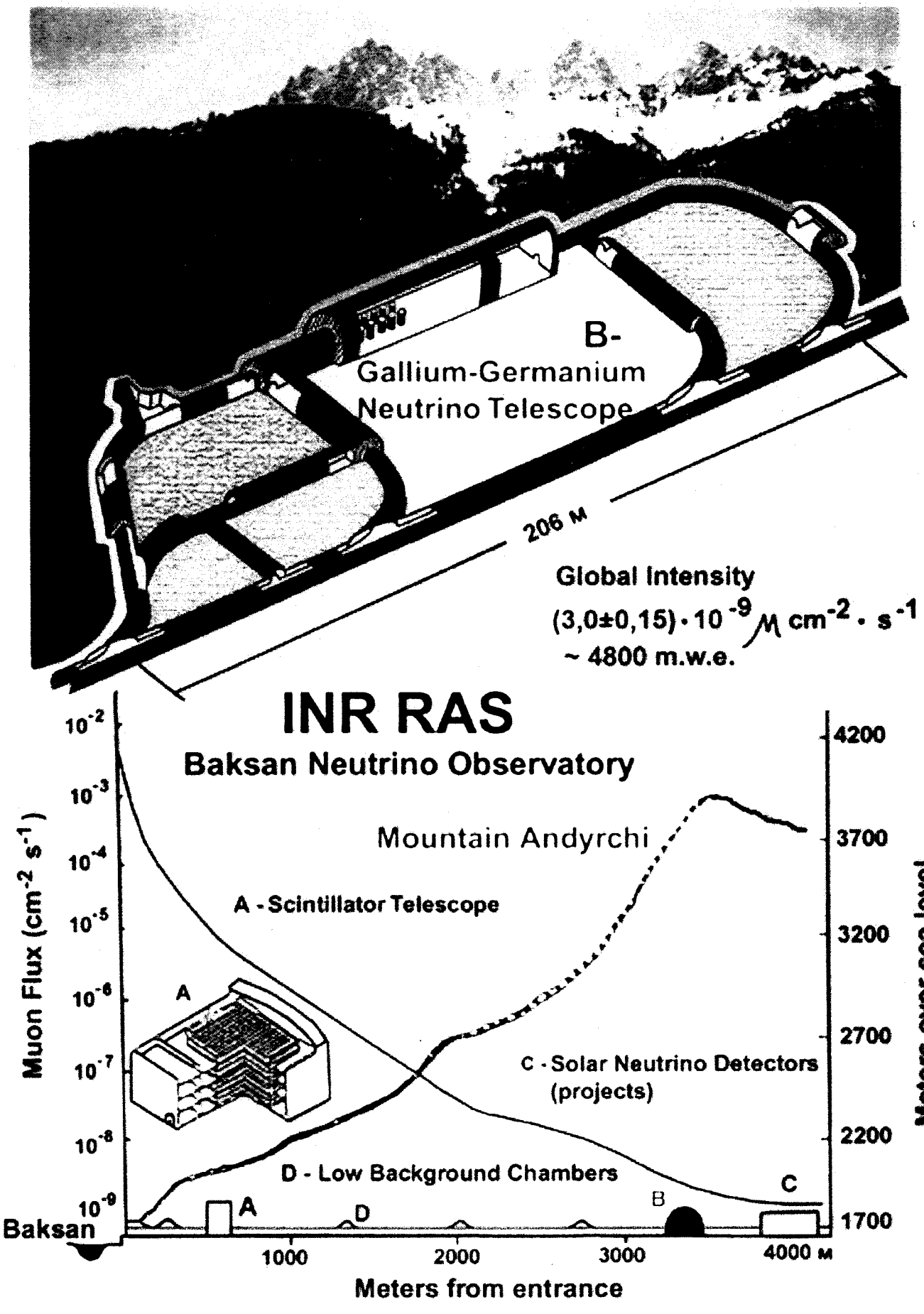
B-
Gallium-Germanium
Neutrino Telescope
206 м
Global Intensity
(3,0±0,15)·10 -9 м cm-2 · s-1
~ 4800 m.w.e.
INR RAS
Baksan Neutrino Observatory
Mountain Andyrchi
A - Scintillator Telescope
A
C - Solar Neutrino Detectors
(projects)
D - Low Background Chambers
Baksan
A
D
B
C
Muon Flux (cm-2 s-1)
Meters over sea level
Meters from entrance
1000
2000
3000
4000 м
4200
3700
3200
2700
2200
1700

GALLIUM-EXPERIMENTS
GALLEX / GNO

$$\nu_e + {}^{71}Ga \rightarrow {}^{71}Ge + e^-$$

i = 39.6 % ; $T_{1/2}$ = 11.43 days
threshold energy: 233 keV

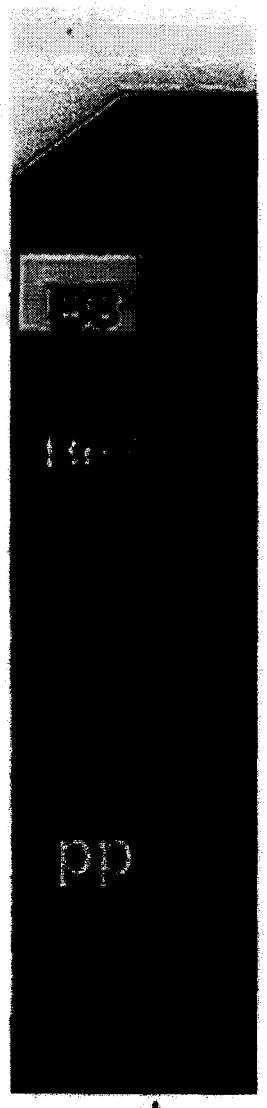

SSM-Expectation:

$130 \pm {}^{9}_{7}$ SNU (1σ) [B.G.P.01]new ^{8}B

[1 SNU = solar neutrino unit = 10^{-36} captures per target nucleus per second]

55.8 % from pp - ν (incl.pep) (72.5 SNU)

26.3 % from ^{7}Be (34.2 SNU)

7% from CNO - ν (9 SNU); 11 % from ^{8}B (14 SNU)

100 tons of aqueous Gallium chloride solution (= 30.3 t Gallium);

correspond to a SSM-production rate of 1.18 atoms of ^{71}Ge per day or ≈14 atoms at the end of a 3-week exposure

Extraction every 3 - 4 weeks , ε ≅ 99 %

Super-Kamiokande dete

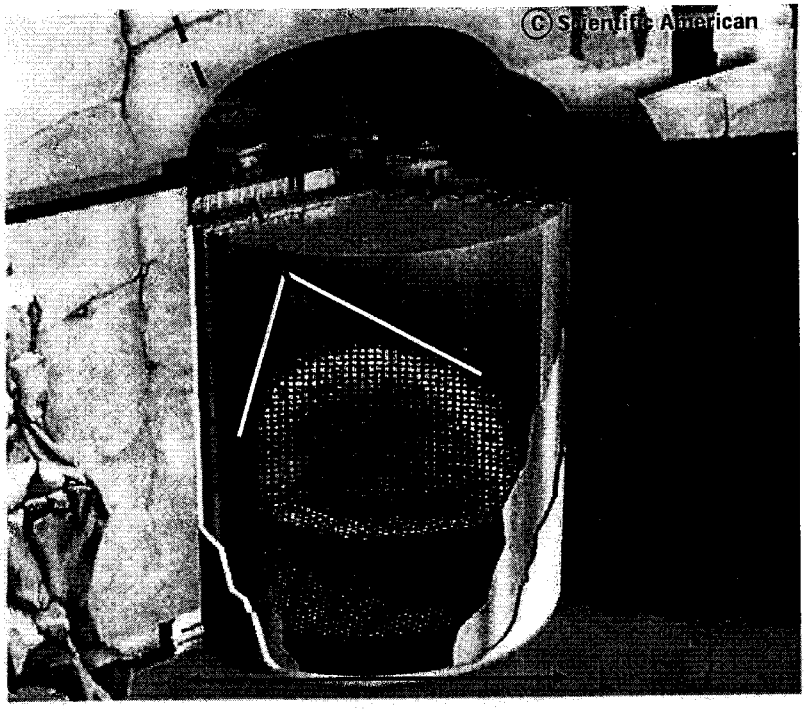

Water Cherenkov detector

. 1000 m underground
. 50,000 ton (22,500 ton fid.)
. inner-detector(ID): 11,146 20 inch PMTs(SK-I)
. outer-detector(OD): 1,885 8 inch PMTs

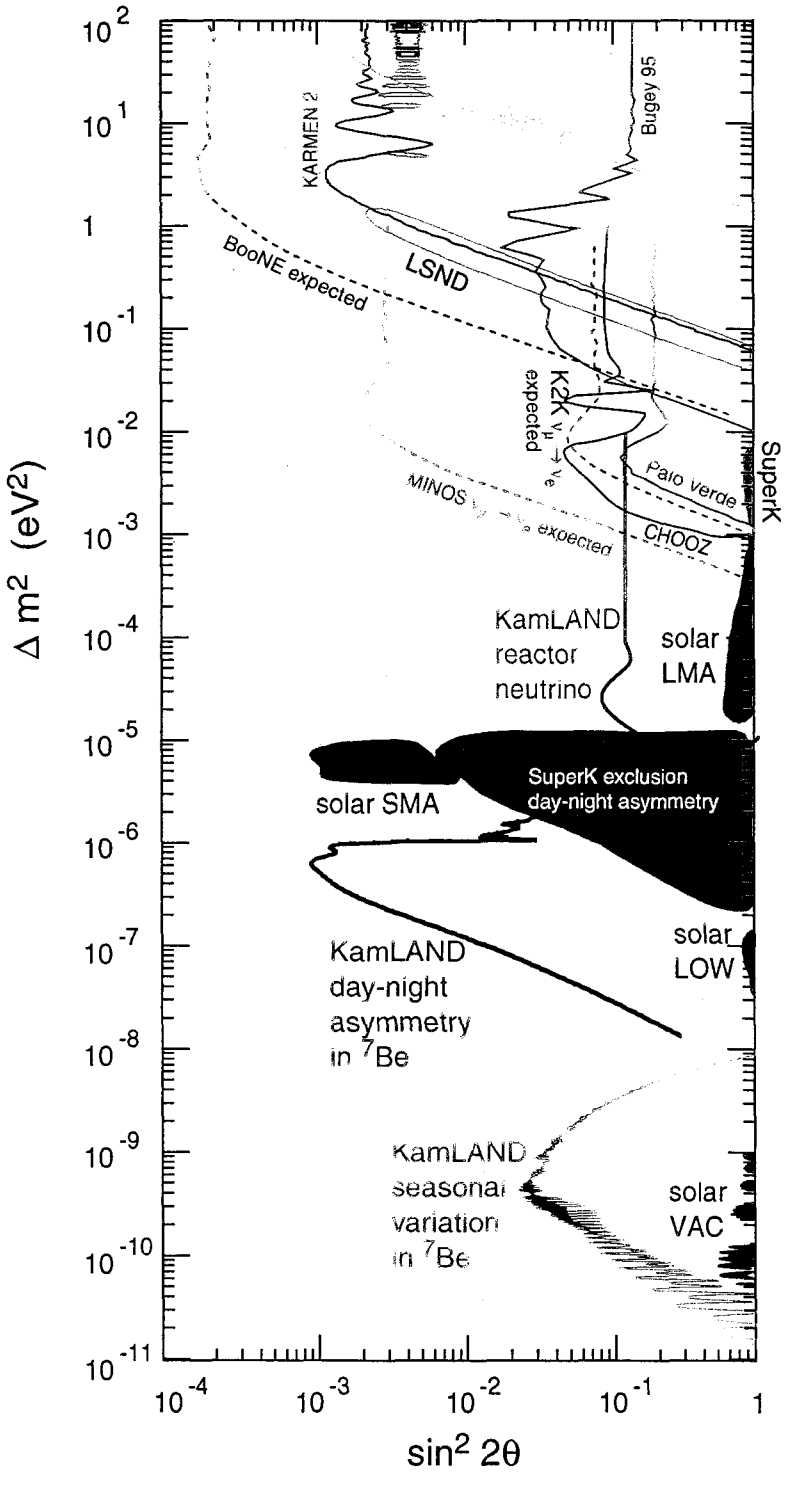

Figure 14: The current and expected limits at some of the future neutrino oscillation experiments. Note that different oscillation modes are shown together.

(M. AKASTEV, S.I.F. '89)

ν - e⁻ Super K

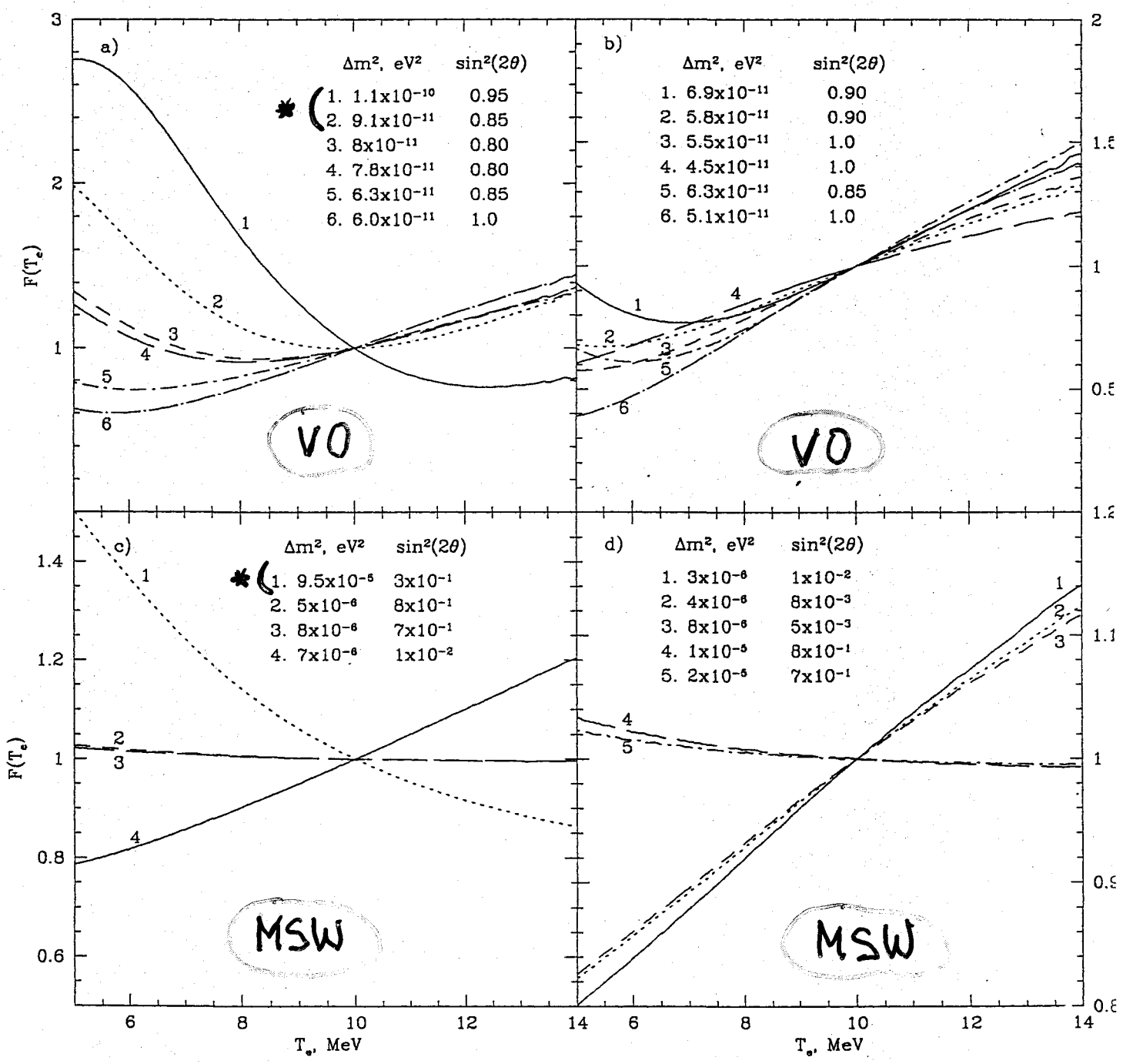

Fig.6

* RULED OUT

(SK '00)

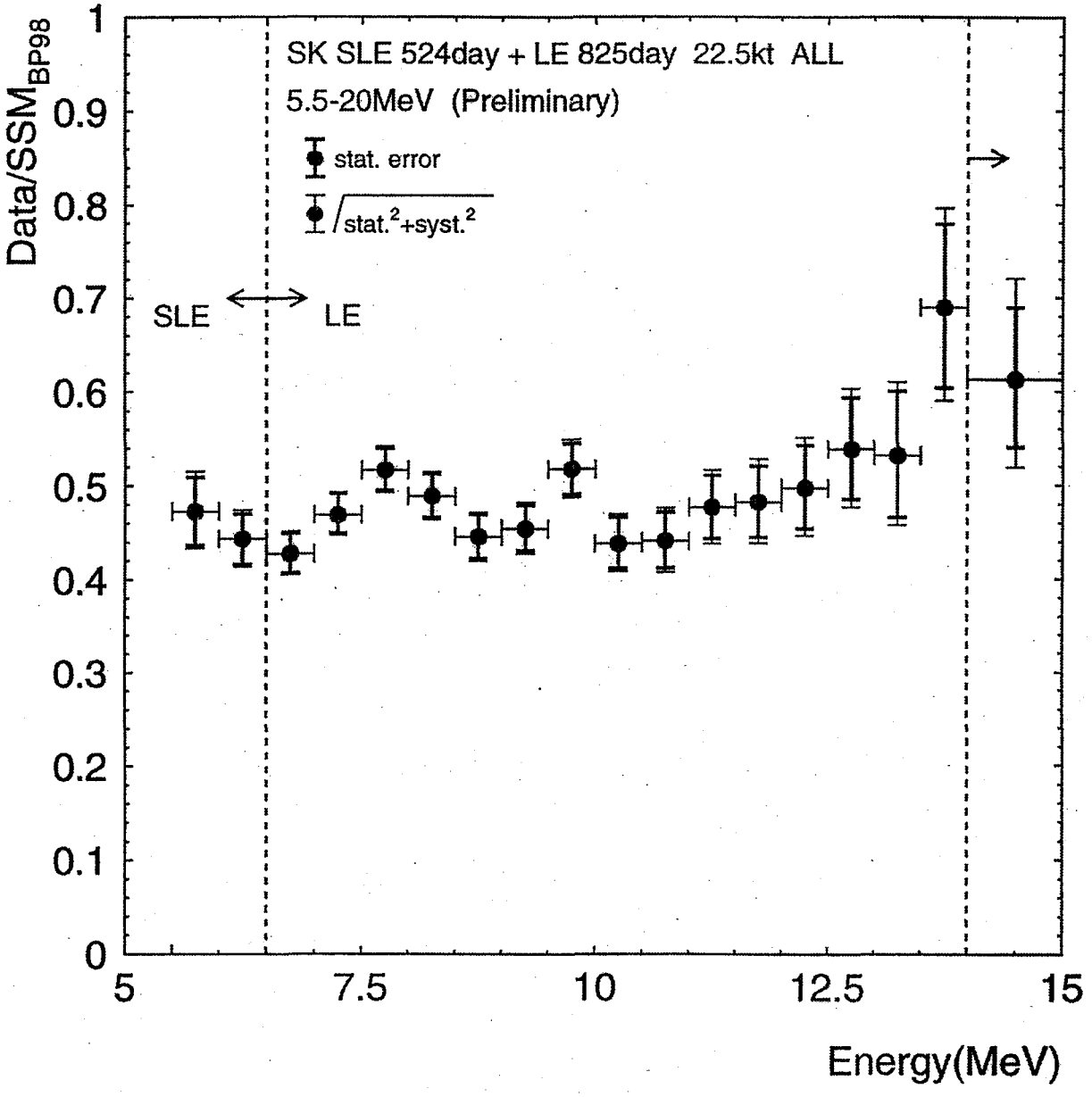
SK SLE 524day + LE 825day 22.5kt ALL
5.5-20MeV (Preliminary)
stat. error
√(stat.²+syst.²)
SLE
LE
Data/SSM_BP98
Energy(MeV)
0
0.1
0.2
0.3
0.4
0.5
0.6
0.7
0.8
0.9
1
5
7.5
10
12.5
15

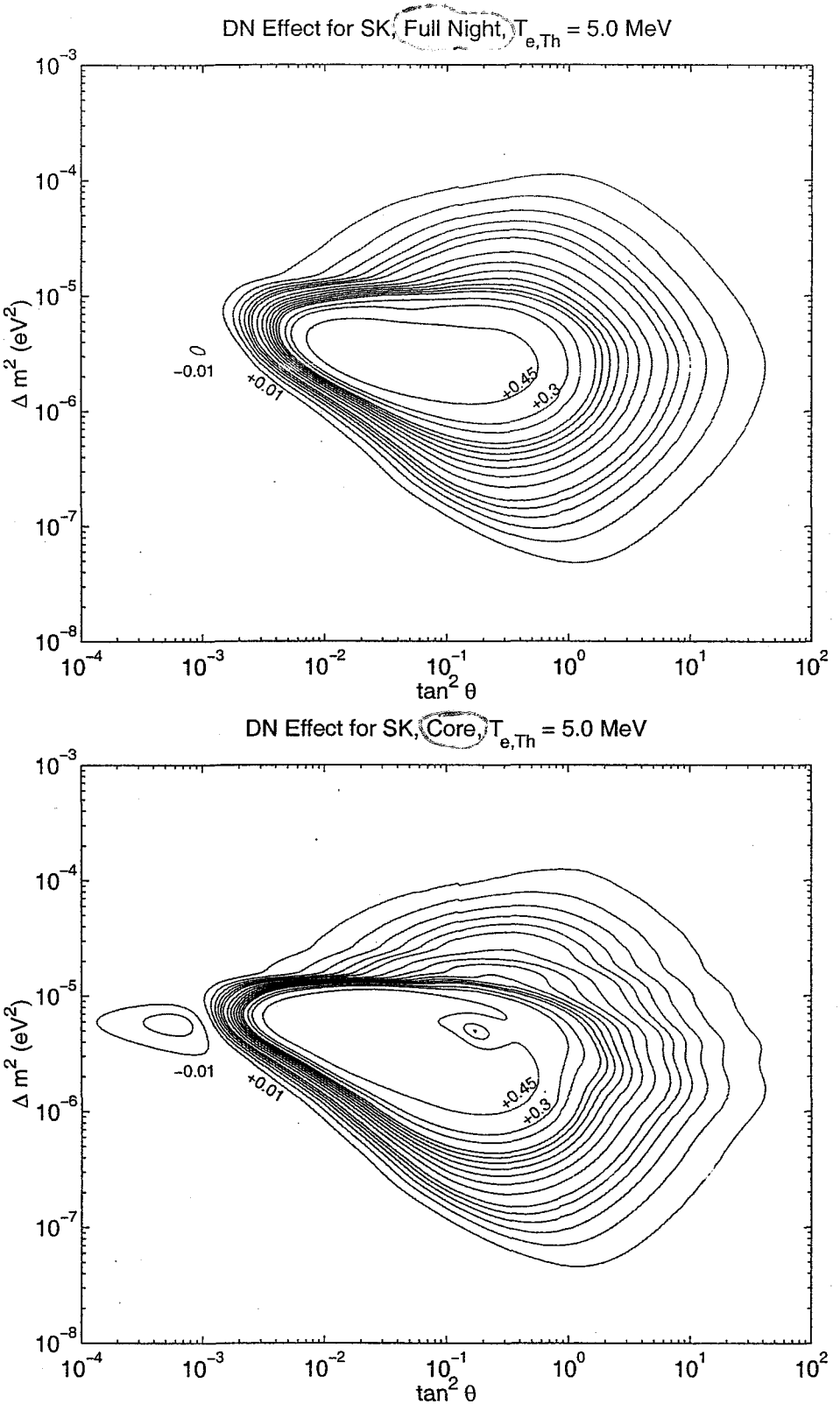

Figure 1: Iso-(D-N) asymmetry contour plot for the Super-Kamiokande experiment for $T_{\mathrm{e,th}} = 5$ MeV, $T_{\mathrm{e,th}}$ being the detected e^- kinetic energy threshold. The contours correspond to values of the *Full Night* (upper panel) and *Core* (lower panel) asymmetries $A_{D-N}^{N,C}(SK) = -0.02,\ -0.01,\ 0.01,\ 0.02,\ 0.03,\ldots,\ 0.09,\ 0.10$.

Daily Variation of SK Rate

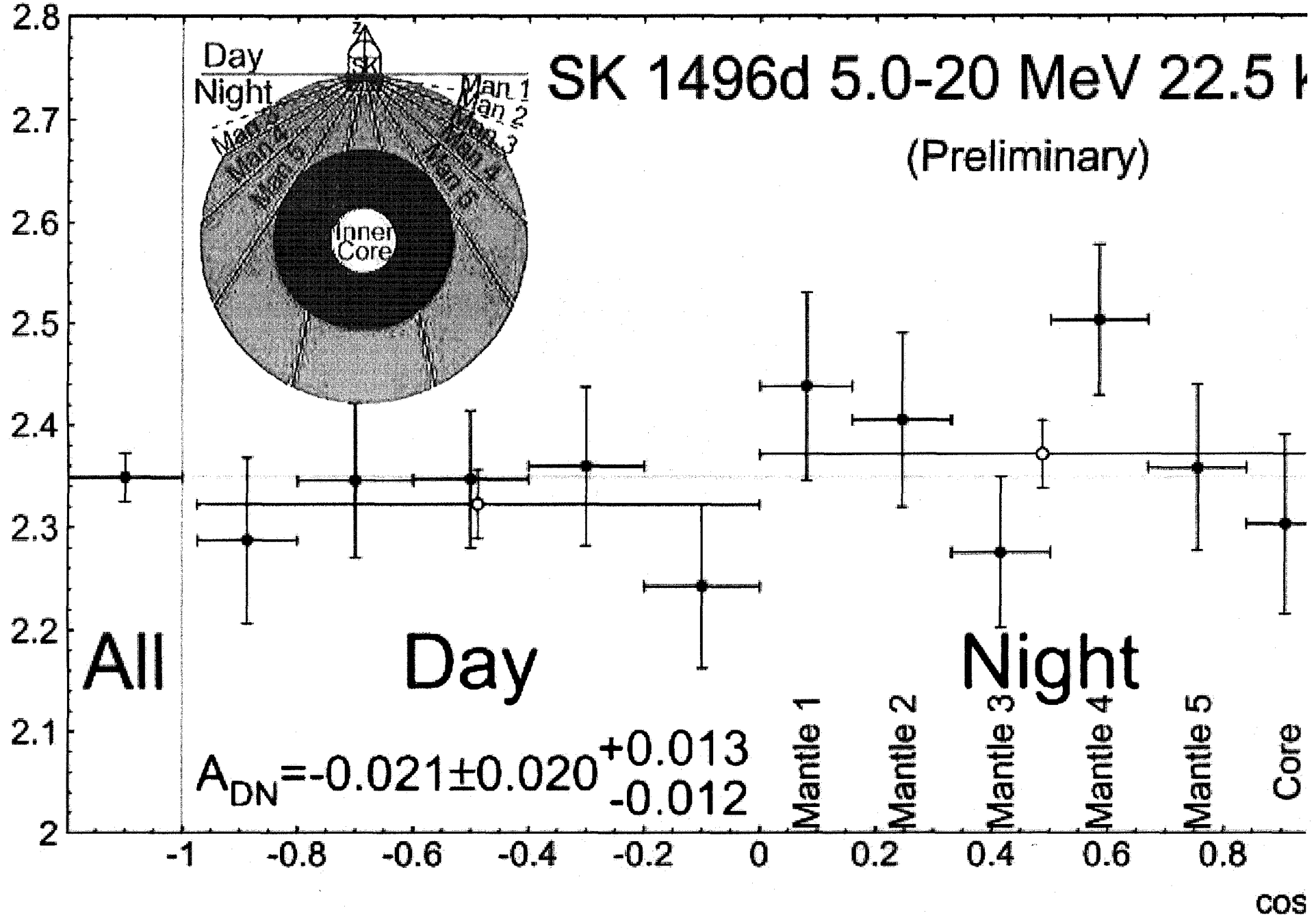

Measurement of charged current interactions produced by ^{8}B solar neutrinos at the Sudbury Neutrino Observatory

Q.R. Ahmad[15], R.C. Allen[11], T.C. Andersen[12], J.D. Anglin[7], G. Bühler[11], J.C. Barton[13‡], E.W. Beier[14], M. Bercovitch[7], J. Bigu[4], S. Biller[13], R.A. Black[13], I. Blevis[2], R.J. Boardman[13], J. Boger[1], E. Bonvin[9], M.G. Boulay[9], M.G. Bowler[13], T.J. Bowles[6], S.J. Brice[6,13], M.C. Browne[15], T.V. Bullard[15], T.H. Burritt[15,6], K. Cameron[12], J. Cameron[13], Y.D. Chan[5], M. Chen[9], H.H. Chen[11*], X. Chen[5,13], M.C. Chon[12], B.T. Cleveland[13], E.T.H. Clifford[9,3], J.H.M. Cowan[4], D.F. Cowen[14], G.A. Cox[15], Y. Dai[9], X. Dai[13], F. Dalnoki-Veress[2], W.F. Davidson[7], P.J. Doe[15,11,6], G. Doucas[13], M.R. Dragowsky[6,5], C.A. Duba[15], F.A. Duncan[9], J. Dunmore[13], E.D. Earle[9,3], S.R. Elliott[15,6], H.C. Evans[9], G.T. Ewan[9], J. Farine[2], H. Fergani[13], A.P. Ferraris[13], R.J. Ford[9], M.M. Fowler[6], K. Frame[13], E.D. Frank[14], W. Frati[14], J.V. Germani[15,6], S. Gil[10], A. Goldschmidt[6], D.R. Grant[2], R.L. Hahn[1], A.L. Hallin[9], E.D. Hallman[4], A. Hamer[6,9], A.A. Hamian[15], R.U. Haq[4], C.K. Hargrove[2], P.J. Harvey[9], R. Hazama[15], R. Heaton[9], K.M. Heeger[15], W.J. Heintzelman[14], J. Heise[10], R.L. Helmer[10†], J.D. Hepburn[9,3], H. Heron[13], J. Hewett[4], A. Hime[6], M. Howe[15], J.G. Hykawy[4], M.C.P. Isaac[5], P. Jagam[12], N.A. Jelley[13], C. Jillings[9], G. Jonkmans[4,3], J. Karn[12], P.T. Keener[14], K. Kirch[6], J.R. Klein[14], A.B. Knox[13], R.J. Komar[10,9], R. Kouzes[8], T. Kutter[10], C.C.M. Kyba[14], J. Law[12], I.T. Lawson[12], M. Lay[13], H.W. Lee[9], K.T. Lesko[5], J.R. Leslie[9], I. Levine[2], W. Locke[13], M.M. Lowry[8], S. Luoma[4], J. Lyon[13], S. Majerus[13], H.B. Mak[9], A.D. Marino[5], N. McCauley[13], A.B. McDonald[9,8], D.S. McDonald[14], K. McFarlane[2], G. McGregor[13], W. McLatchie[9], R. Meijer Drees[15], H. Mes[2], C. Mifflin[2], G.G. Miller[6], G. Milton[3], B.A. Moffat[9], M. Moorhead[13], C.W. Nally[10], M.S. Neubauer[14], F.M. Newcomer[14], H.S. Ng[10], A.J. Noble[2†], E.B. Norman[5], V.M. Novikov[2], M. O'Neill[2], C.E. Okada[5], R.W. Ollerhead[12], M. Omori[13], J.L. Orrell[15], S.M. Oser[14], A.W.P. Poon[5,6,10,15], T.J. Radcliffe[9], A. Roberge[4], B.C. Robertson[9], R.G.H. Robertson[15,6], J.K. Rowley[1], V.L. Rusu[14], E. Saettler[4], K.K. Schaffer[15], A. Schuelke[5], M.H. Schwendener[4], H. Seifert[4,6,15], M. Shatkay[2], J.J. Simpson[12], D. Sinclair[2], P. Skensved[9], A.R. Smith[5], M.W.E. Smith[15], N. Starinsky[2], T.D. Steiger[15], R.G. Stokstad[5], R.S. Storey[7*], B. Sur[3,9], R. Tafirout[4], N. Tagg[12], N.W. Tanner[13], R.K. Taplin[13], M. Thorman[13], P. Thornewell[6,13,15] P.T. Trent[13‡], Y.I. Tserkovnyak[10], R. Van Berg[14], R.G. Van de Water[14,6], C.J. Virtue[4], C.E. Waltham[10], J.-X. Wang[12], D.L. Wark[13,6§], N. West[13], J.B. Wilhelmy[6], J.F. Wilkerson[15,6], J. Wilson[13], P. Wittich[14], J.M. Wouters[6], M. Yeh[1]

(The SNO Collaboration)

[1] *Chemistry Department, Brookhaven National Laboratory, Upton, NY 11973-5000*

[2] *Carleton University, Ottawa, Ontario K1S 5B6 Canada*

[3] *Chalk River Laboratories, AECL Research, Chalk River, Ontario K0J 1J0 Canada*

[4] *Department of Physics and Astronomy, Laurentian University, Sudbury, Ontario P3E 2C6 Canada*

[5] *Institute of Nuclear and Particle Astrophysics and Nuclear Science Division, Lawrence Berkeley National Laboratory, Berkeley, CA 94720*

[6] *Los Alamos National Laboratory, Los Alamos, NM 87545*

[7] *National Research Council of Canada, Ottawa, Ontario K1A 0R6 Canada*

[8] *Department of Physics, Princeton University, Princeton, NJ 08544*

[9] *Department of Physics, Queen's University, Kingston, Ontario K7L 3N6 Canada*

[10] *Department of Physics and Astronomy, University of British Columbia, Vancouver, BC V6T 1Z1 Canada*

[11] *Department of Physics, University of California, Irvine, CA 92717*

[12] *Physics Department, University of Guelph, Guelph, Ontario N1G 2W1 Canada*

[13] *Nuclear and Astrophysics Laboratory, University of Oxford, Keble Road, Oxford, OX1 3RH, UK*

[14] *Department of Physics and Astronomy, University of Pennsylvania, Philadelphia, PA 19104-6396,*

[15] *Center for Experimental Nuclear Physics and Astrophysics, and Department of Physics, University of Washington, Seattle, WA 98195*

(18 June 2001)

Solar neutrinos from the decay of ^{8}B have been detected at the Sudbury Neutrino Observatory (SNO) via the charged current (CC) reaction on deuterium and by the elastic scattering (ES) of electrons. The CC reaction is sensitive exclusively to ν_e's, while the ES reaction also has a small sensitivity to ν_μ's and ν_τ's. The flux of ν_e's from ^{8}B decay measured by the CC reaction rate is $\phi^{\rm CC}(\nu_e) = 1.75 \pm 0.07\ (\text{stat.})^{+0.12}_{-0.11}\ (\text{sys.}) \pm 0.05\ (\text{theor.}) \times 10^6\ \text{cm}^{-2}\text{s}^{-1}$. Assuming no flavor tranformation, the flux inferred from the ES reaction rate is $\phi^{\rm ES}(\nu_x) = 2.39 \pm 0.34\ (\text{stat.})^{+0.16}_{-0.14}\ (\text{sys.}) \times 10^6\ \text{cm}^{-2}\text{s}^{-1}$. Comparison of $\phi^{\rm CC}(\nu_e)$ to the Super-Kamiokande Collaboration's precision value of $\phi^{\rm ES}(\nu_x)$ yields a 3.3σ difference, providing evidence that there is a non-electron flavor active neutrino component in the solar flux. The total flux of active ^{8}B neutrinos is thus determined to be $5.44 \pm 0.99 \times 10^6\ \text{cm}^{-2}\text{s}^{-1}$, in close agreement with the predictions of solar models.

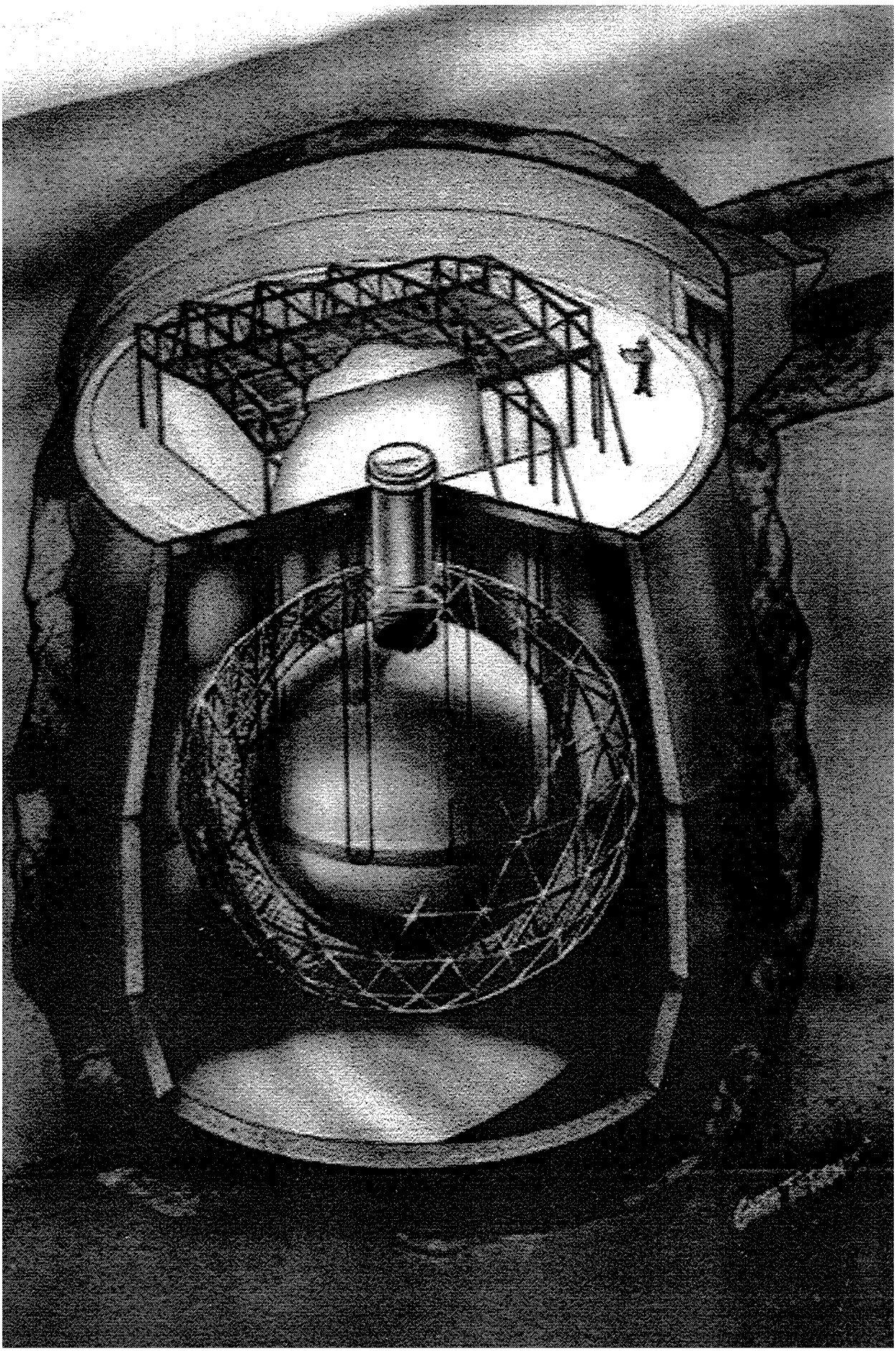

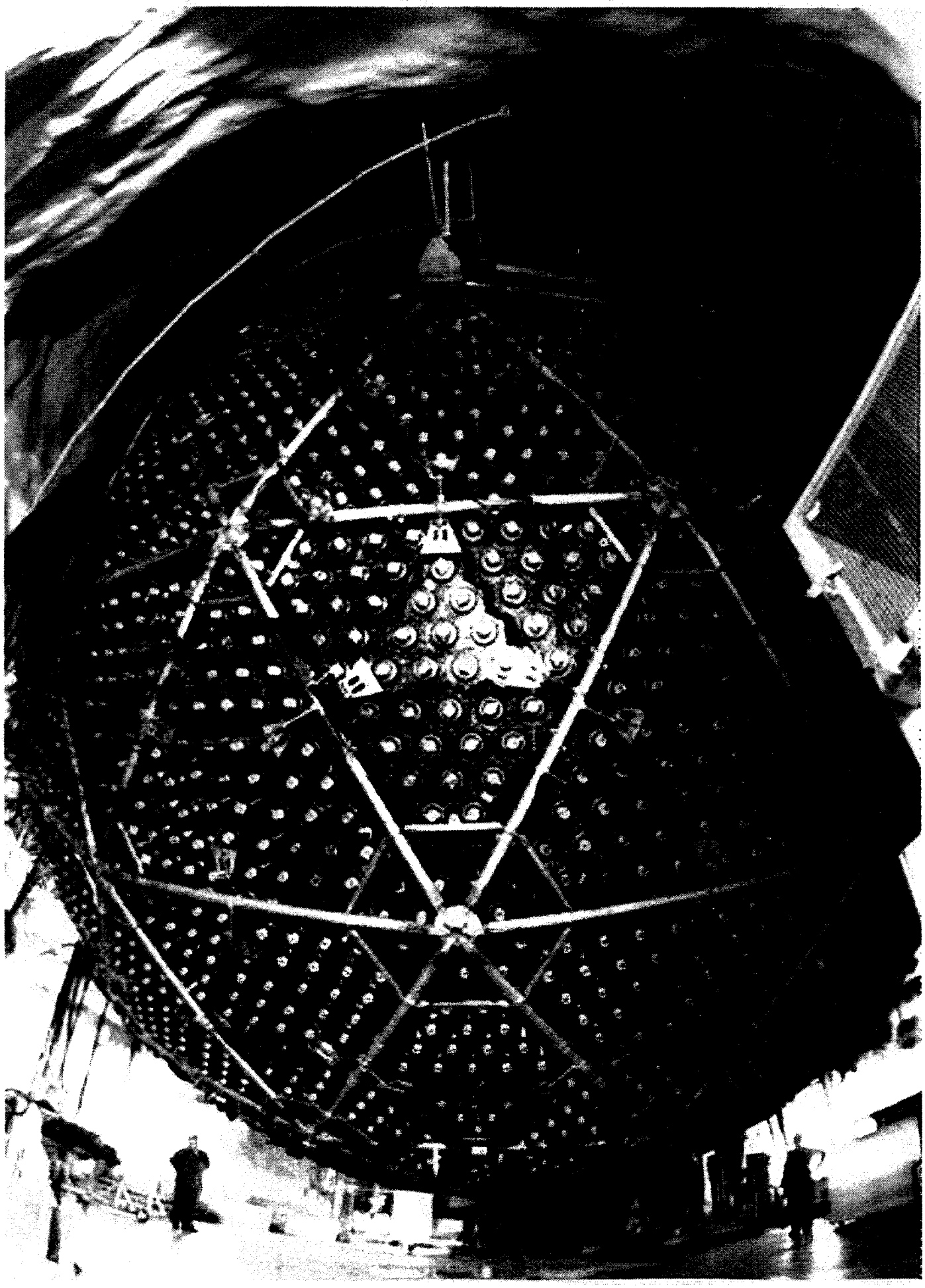

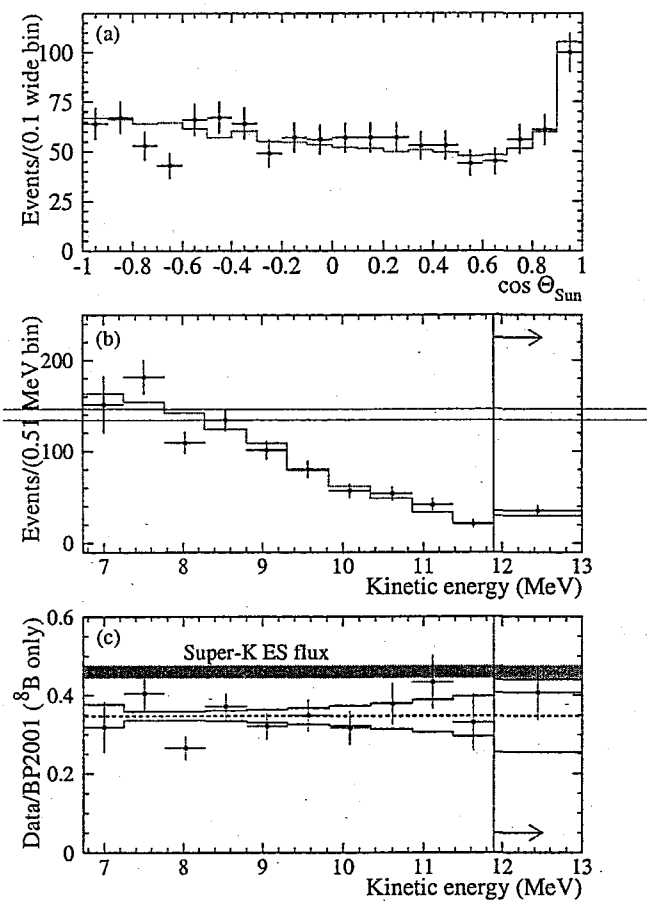

FIG. 2. Distributions of (a) $\cos\theta_\odot$, and (b) Extracted kinetic energy spectrum for CC events with R $\leq$5.50 m and $T_{\rm eff}\geq$6.75 MeV. The Monte Carlo simulations for an undistorted ^{8}B spectrum are shown as histograms. The ratio of the data to the expected kinetic energy distribution with correlated systematic errors is shown in (c).

sources of systematic uncertainty in this signal extraction are the energy scale uncertainty and reconstruction accuracy, as shown in Table II. The CC and ES signal decomposition gives consistent results when used with the $N_{\rm hit}$ energy estimator, as well as with different choices of the analysis threshold and the fiducial volume up to 6.20 m with backgrounds characterized by pdfs.

The CC spectrum can be extracted from the data by removing the constraint on the shape of the CC pdf and repeating the signal extraction. Figure 2 (b) shows the kinetic energy spectrum with statistical error bars with the predicted standard ^{8}B spectrum [7] superimposed. The ratio of the data to the prediction is shown in Figure 2 (c). The bands represent the 1σ uncertainties derived from the most significant energy-dependent systematic errors. There is no evidence for a deviation of the spectral shape from the predicted shape under the non-oscillation hypothesis.

TABLE II. Systematic error on fluxes.

Error source	CC error (percent)	ES error (per cent)
Energy scale	-5.2, +6.1	-3.5 ,+5.4
Energy resolution	±0.5	±0.3
Energy scale non-linearity	±0.5	±0.4
Vertex accuracy	±3.1	±3.3
Vertex resolution	±0.7	±0.4
Angular resolution	±0.5	±2.2
High energy γ's	-0.8, +0.0	-1.9, +0.0
Low energy background	-0.2, +0.0	-0.2, +0.0
Instrumental background	-0.2, +0.0	-0.6, +0.0
Trigger efficiency	0.0	0.0
Live time	±0.1	±0.1
Cut acceptance	-0.6, +0.7	-0.6, +0.7
Earth orbit eccentricity	±0.2	±0.2
^{17}O, ^{18}O	0.0	0.0
Experimental uncertainty	-6.2, +7.0	-5.7, +6.8
Cross section	3.0	0.5
Solar Model	-16, +20	-16, +20

Using the integrated rates above the kinetic energy threshold $T_{\rm eff}$ = 6.75 MeV, the measured ^{8}B neutrino fluxes assuming no oscillations are:

$$\phi^{\rm CC}_{\rm SNO}(\nu_e) = 1.75 \pm 0.07\ ({\rm stat.})^{+0.12}_{-0.11}\ ({\rm sys.}) \pm 0.05\ ({\rm theor.}) \times 10^6\ {\rm cm}^{-2}{\rm s}^{-1}$$

$$\phi^{\rm ES}_{\rm SNO}(\nu_x) = 2.39 \pm 0.34({\rm stat.})^{+0.16}_{-0.14}\ ({\rm sys.}) \times 10^6\ {\rm cm}^{-2}{\rm s}^{-1}$$

where the theoretical uncertainty is the CC cross section uncertainty [10]. Radiative corrections have not been applied to the CC cross section, but they are expected to decrease the measured $\phi^{\rm CC}(\nu_e)$ flux [14] by up to a few percent. The difference between the ^{8}B flux deduced from the ES rate and that deduced from the CC rate in SNO is $0.64 \pm 0.40 \times 10^6$ cm^{-2}s^{-1}, or 1.6σ. SNO's ES rate measurement is consistent with the precision measurement by the Super-Kamiokande Collaboration of the ^{8}B flux using the same ES reaction [5]:

$$\phi^{\rm ES}_{\rm SK}(\nu_x) = 2.32 \pm 0.03\ ({\rm stat.})^{+0.08}_{-0.07}\ ({\rm sys.}) \times 10^6\ {\rm cm}^{-2}{\rm s}^{-1}.$$

The difference between the flux $\phi^{\rm ES}(\nu_x)$ measured by Super-Kamiokande via the ES reaction and the $\phi^{CC}(\nu_e)$ flux measured by SNO via the CC reaction is $0.57 \pm 0.17 \times 10^6$ cm^{-2}s^{-1}, or 3.3σ [8]. The probability that the SNO measurement is not a downward fluctuation from the Super-Kamiokande measurement is 99.96%. For reference, the ratio of the SNO CC ^{8}B flux to that of the BP2001 solar model [7] is 0.347±0.029, where all uncertainties are added in quadrature.

If oscillation with maximal mixing to a sterile neutrino is occurring, the SNO CC-derived ^{8}B flux above a threshold of 6.75 MeV will be consistent with the integrated Super-Kamiokande ES-derived ^{8}B flux above a

threshold of 8.5 MeV [20]. Correcting for the ES threshold [5] this derived flux difference is $0.53 \pm 0.17 \times 10^6$ $\mathrm{cm}^{-2}\mathrm{s}^{-1}$, or 3.1σ. The probability that this difference is not a downward fluctuation is 99.87%. These data are therefore evidence of a non-electron active flavor component in the solar neutrino flux. These data are also inconsistent with the "Just-So^2" parameters for neutrino oscillation [15].

Figure 3 displays the inferred flux of non-electron flavor active neutrinos ($\phi(\nu_{\mu\tau})$) against the flux of electron neutrinos. The two data bands represent the one standard deviation measurements of the SNO CC rate and the Super-Kamiokande ES rate. The error ellipses represent the 68%, 95%, and 99% joint probability contours for $\phi(\nu_e)$ and ($\phi(\nu_{\mu\tau})$). The best fit to $\phi(\nu_{\mu\tau})$ is:

$$\phi(\nu_{\mu\tau}) = 3.69 \pm 1.13 \times 10^6 \text{ cm}^{-2}\text{s}^{-1}.$$

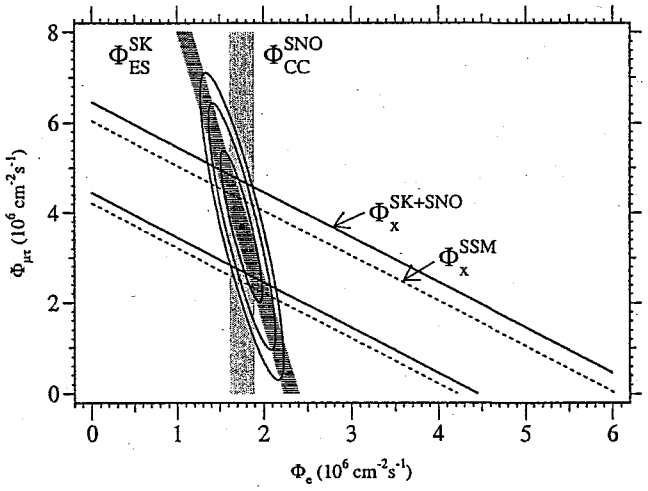

FIG. 3. Flux of ^{8}B solar neutrinos which are μ or τ flavor vs. the flux of electron neutrinos as deduced from the SNO and Super-Kamiokande data. The diagonal bands show the total ^{8}B flux $\phi(\nu_x)$ as predicted by BP2001 (dashed lines) and that derived from the SNO and Super-Kamiokande measurements (solid lines). The intercepts of these bands with the axes represent the $\pm 1\sigma$ errors.

The total flux of active ^{8}B neutrinos is determined to be:

$$\phi(\nu_x) = 5.44 \pm 0.99 \times 10^6 \text{ cm}^{-2}\text{s}^{-1}.$$

This result is displayed as a diagonal band in Fig. 3, and is in excellent agreement with predictions of standard solar models [7,9].

The evidence for electron neutrino flavor change implies a mass squared difference between ν_e and ν_μ or ν_τ that is less than 10^{-3} eV^2 as shown by previous analyses [16,15]. This result can also be combined with present limits on electron neutrino mass [17] of less than 2.8 eV and $\Delta m^2_{\mu\tau}$ (assuming neutrino oscillations [19]), to limit the sum of the masses of ν_e, ν_μ, and ν_τ to be between 0.05 and 8.4 eV. This corresponds to a constraint of $0.001 < \Omega_\nu < 0.18$ for the neutrino mass contribution to the critical density of the Universe [18].

In summary, the results presented here are the first direct indication of a non-electron flavor component in the solar neutrino flux, and enable the first determination of the total flux of ^{8}B neutrinos generated by the Sun.

This research was supported by the Canadian Natural Sciences and Engineering Research Council of Canada, Industry Canada, National Research Council of Canada, Northern Ontario Heritage Fund Corporation and the Province of Ontario, the United States Department of Energy, and the United Kingdom by the Science and Engineering Research Council and the Particle Physics and Astronomy Research Council. Further support was provided by INCO, Ltd., Atomic Energy of Canada Limited (AECL), Agra-Monenco, Canatom, Canadian Microelectronics Corporation, AT&T Microelectronics, Northern Telecom and British Nuclear Fuels, Ltd. The heavy water was loaned by AECL with the cooperation of Ontario Power Generation.

* Deceased.
† Permanent address: TRIUMF, 4004 Wesbrook Mall, Vancouver, BC V6T 2A3, Canada.
‡ Permanent address: Birkbeck College, University of London, Malet Road, London WC1E 7HX, UK.
§ Permanent address: Rutherford Appleton Laboratory, Chilton, Didcot, Oxon, OX11 0QX, and University of Sussex, Physics and Astronomy Department, Brighton BN1 9QH, UK.

[1] B.T. Cleveland *et al.*, Astrophys. J. **496**, 505 (1998).
[2] K.S. Hirata *et al.*, Phys. Rev. Lett. **65**, 1297 (1990); K.S. Hirata *et al.*, Phys. Rev. D **44**, 2241 (1991); Y. Fukuda *et al.*, Phys. Rev. Lett. **77**, 1683 (1996).
[3] J.N. Abdurashitov *et al.*, Phys. Rev. C **60**, 055801, (1999).
[4] W. Hampel *et al.*, Phys. Lett. B **447**, 127 (1999).
[5] S. Fukuda *et al.*, Phys. Rev. Lett. **86**, 5651 (2001).
[6] W. Altmann *et al.*, Phys. Lett. B **490**, 16 (2000).
[7] J.N. Bahcall, M. H. Pinsonneault, and S. Basu, astro-ph/0010346 v2. The reference ^{8}B neutrino flux is 5.05×10^6 cm^{-2}s^{-1}.
[8] Given the limit set for the *hep* flux by Ref. [5], the effects of the *hep* contribution may increase this difference by a few percent.
[9] A.S. Brun, S. Turck-Chièze, and J.P. Zahn, Astrophys. J. **525**, 1032 (1999).

SK : $\nu + e^- \to \nu + e^-$

$\nu_\odot$: $\nu_e \longrightarrow \nu_{\mu,\tau}$

$$R(SK) : \phi(\nu_\odot)\left[P(\nu_e \to \nu_e)\sigma(\nu_e e^-) + P(\nu_e \to \nu_{\mu,\tau})\sigma(\nu_\mu e^-)\right]$$

$$\sigma(\nu_\mu e^-) = \sigma(\nu_\tau e^-) \simeq \frac{1}{6}\sigma(\nu_e e^-)$$

$$P(\nu_e \to \nu_e) + P(\nu_e \to \nu_\mu) + P(\nu_e \to \nu_\tau) = 1$$

$$R(SK) : \left[\underbrace{\Phi_E(\nu_e)} + \frac{1}{6}\underbrace{\Phi_E(\nu_{\mu,\tau})}\right]\sigma(\nu_e e^-)$$

$$\Phi_E(\nu_e) = \phi(\nu_\odot)_{^8B} P(\nu_e \to \nu_e)$$

$$\Phi_E(\nu_{\mu,\tau}) = \phi(\nu_\odot)\left[1 - P(\nu_e \to \nu_e)\right]$$

SNO:

$$\Phi(\nu_e) = 1.75 \pm 0.15 \times 10^6 \, cm^{-2} s^{-1}$$

$$\Phi(\nu_{\mu,\tau}) = 3.69 \pm 1.17 \times 10^6 \, cm^{-2} s^{-1}$$

$$\frac{\Phi(\nu_e)}{\Phi(\nu_e) + \Phi(\nu_{\mu,\tau})} = 0.32 \pm 0.07$$

$$= \frac{R^{CC}_{SNO} / R^{NC}_{SNO}}{(R^{CC}_{SNO} / R^{NC}_{SNO})_{SSM}}$$

$$R^{CC/NC} = 0.25 - 0.39$$

$$0.18 - 0.46$$

TABLE II: Systematic uncertainties on fluxes. The experimental uncertainty for ES (not shown) is -4.8,+5.0 percent. † denotes CC vs NC anti-correlation.

Source	CC Uncert. (percent)	NC Uncert. (percent)	$\phi_{\mu\tau}$ Uncert. (percent)
Energy scale †	-4.2,+4.3	-6.2,+6.1	-10.4,+10.3
Energy resolution †	-0.9,+0.0	-0.0,+4.4	-0.0,+6.8
Energy non-linearity †	±0.1	±0.4	±0.6
Vertex resolution †	±0.0	±0.1	±0.2
Vertex accuracy	-2.8,+2.9	±1.8	±1.4
Angular resolution	-0.2,+0.2	-0.3,+0.3	-0.3,+0.3
Internal source pd †	±0.0	-1.5,+1.6	-2.0,+2.2
External source pd	±0.1	-1.0,+1.0	±1.4
D_2O Cherenkov †	-0.1,+0.2	-2.6,+1.2	-3.7,+1.7
H_2O Cherenkov	±0.0	-0.2,+0.4	-0.2,+0.6
AV Cherenkov	±0.0	-0.2,+0.2	-0.3,+0.3
PMT Cherenkov †	±0.1	-2.1,+1.6	-3.0,+2.2
Neutron capture	±0.0	-4.0,+3.6	-5.8,+5.2
Cut acceptance	-0.2,+0.4	-0.2,+0.4	-0.2,+0.4
Experimental uncertainty	-5.2,+5.2	-8.5,+9.1	-13.2,+14.1
Cross section [7]	±1.8	±1.3	±1.4

2928 events in the energy region selected for analysis, 5 to 20 MeV. Fig. 2(a) shows the distribution of selected events in the cosine of the angle between the Cherenkov event direction and the direction from the sun ($\cos\theta_\odot$) for the analysis threshold of $T_{\rm eff} \geq$ 5 MeV and fiducial volume selection of $R \leq 550$ cm, where R is the reconstructed event radius. Fig. 2(b) shows the distribution of events in the volume-weighted radial variable $(R/R_{\rm AV})^3$, where $R_{\rm AV} = 600$ cm is the radius of the acrylic vessel. Figure 2(c) shows the kinetic energy spectrum of the selected events.

In order to test the null hypothesis, the assumption that there are only electron neutrinos in the solar neutrino flux, the data are resolved into contributions from CC, ES, and NC events above threshold using pdfs in $T_{\rm eff}$, $\cos\theta_\odot$, and $(R/R_{\rm AV})^3$, derived from Monte Carlo calculations generated assuming no flavor transformation and the standard ^{8}B spectral shape [6]. Background event pdfs are included in the analysis with fixed amplitudes determined by the background calibration. The extended maximum likelihood method used in the signal decomposition yields $1967.7^{+61.9}_{-60.9}$ CC events, $263.6^{+26.4}_{-25.6}$ ES events, and $576.5^{+49.5}_{-48.9}$ NC events [12], where only statistical uncertainties are given. Systematic uncertainties on fluxes derived by repeating the signal decomposition with perturbed pdfs (constrained by calibration data) are shown in Table II.

Normalized to the integrated rates above the kinetic energy threshold of $T_{\rm eff} \geq$ 5 MeV, the flux of ^{8}B neutrinos measured with each reaction in SNO, assuming the standard spectrum shape [6] is (all fluxes are presented in units of 10^6 cm^{-2}s^{-1}):

$$\phi_{\rm CC}^{\rm SNO} = 1.76^{+0.06}_{-0.05}({\rm stat.})^{+0.09}_{-0.09}\ ({\rm syst.})$$
$$\phi_{\rm ES}^{\rm SNO} = 2.39^{+0.24}_{-0.23}({\rm stat.})^{+0.12}_{-0.12}\ ({\rm syst.})$$
$$\phi_{\rm NC}^{\rm SNO} = 5.09^{+0.44}_{-0.43}({\rm stat.})^{+0.46}_{-0.43}\ ({\rm syst.}).$$

Electron neutrino cross sections are used to calculate all

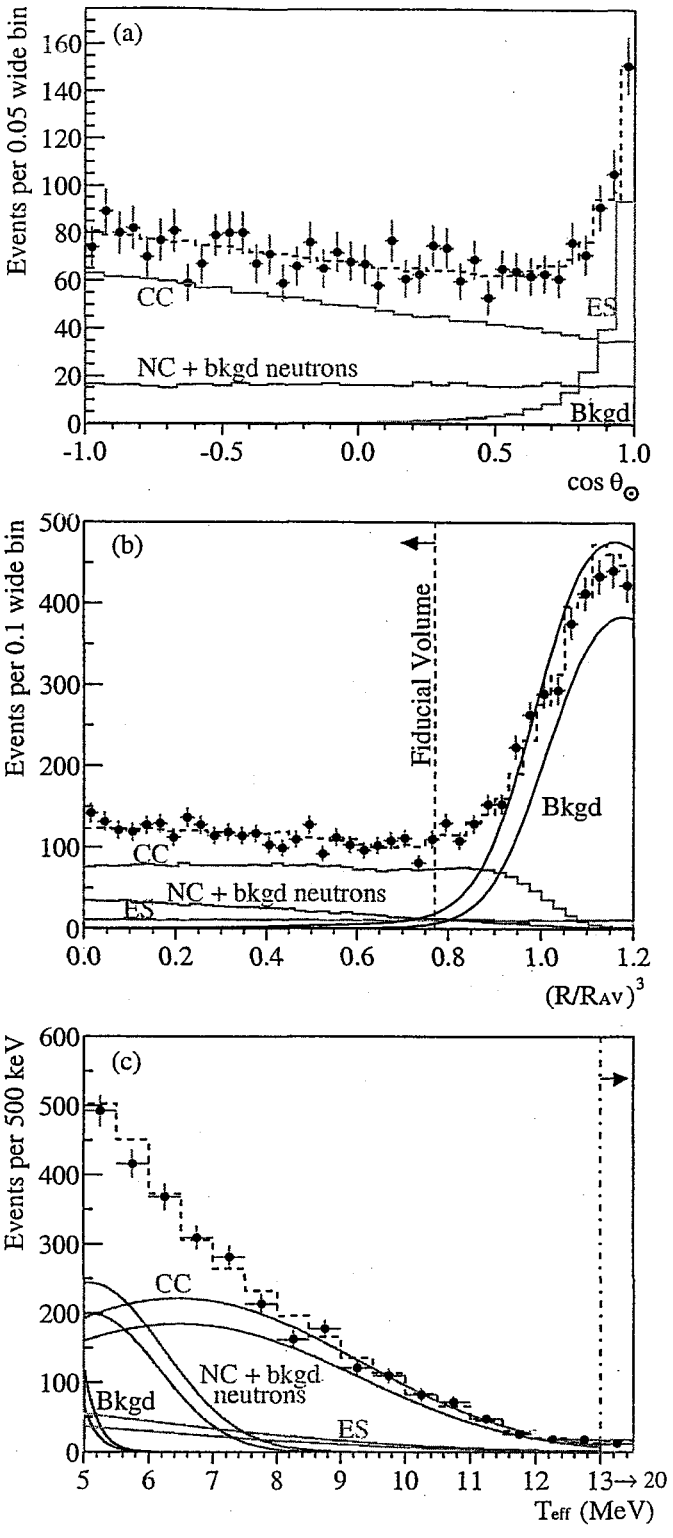

FIG. 2: (a) Distribution of $\cos\theta_\odot$ for $R \leq 550$ cm. (b) Distribution of the volume weighted radial variable $(R/R_{\rm AV})^3$. (c) Kinetic energy for $R \leq 550$ cm. Also shown are the Monte Carlo predictions for CC, ES and NC + bkgd neutron events scaled to the fit results, and the calculated spectrum of Cherenkov background (Bkgd) events. The dashed lines represent the summed components, and the bands show $\pm 1\sigma$ uncertainties. All distributions are for events with $T_{\rm eff} \geq$5 MeV.

fluxes. The CC and ES results reported here are consistent with the earlier SNO results [2] for $T_{\rm eff} \geq 6.75$ MeV. The excess of the NC flux over the CC and ES fluxes implies neutrino flavor transformations.

A simple change of variables resolves the data directly into electron (ϕ_e) and non-electron ($\phi_{\mu\tau}$) components [13],

$$\phi_e = 1.76^{+0.05}_{-0.05}(\text{stat.})^{+0.09}_{-0.09}\ (\text{syst.})$$
$$\phi_{\mu\tau} = 3.41^{+0.45}_{-0.45}(\text{stat.})^{+0.48}_{-0.45}\ (\text{syst.})$$

assuming the standard ^{8}B shape. Combining the statistical and systematic uncertainties in quadrature, $\phi_{\mu\tau}$ is $3.41^{+0.66}_{-0.64}$, which is 5.3σ above zero, providing strong evidence for flavor transformation consistent with neutrino oscillations [8, 9]. Adding the Super-Kamiokande ES measurement of the ^{8}B flux [10] $\phi_{\rm ES}^{\rm SK} = 2.32 \pm 0.03(\text{stat.})^{+0.08}_{-0.07}$ (syst.) as an additional constraint, we find $\phi_{\mu\tau} = 3.45^{+0.65}_{-0.62}$, which is 5.5σ above zero. Figure 3 shows the flux of non-electron flavor active neutrinos vs the flux of electron neutrinos deduced from the SNO data. The three bands represent the one standard deviation measurements of the CC, ES, and NC rates. The error ellipses represent the 68%, 95%, and 99% joint probability contours for ϕ_e and $\phi_{\mu\tau}$.

Removing the constraint that the solar neutrino energy spectrum is undistorted, the signal decomposition is repeated using only the $\cos\theta_\odot$ and $(R/R_{\rm AV})^3$ information. The total flux of active ^{8}B neutrinos measured with the NC reaction is

$$\phi_{\rm NC}^{\rm SNO} = 6.42^{+1.57}_{-1.57}(\text{stat.})^{+0.55}_{-0.58}\ (\text{syst.})$$

which is in agreement with the shape constrained value above and with the standard solar model prediction [11] for ^{8}B, $\phi_{\rm SSM} = 5.05^{+1.01}_{-0.81}$.

In summary, the results presented here are the first direct measurement of the total flux of active ^{8}B neutrinos arriving from the sun and provide strong evidence for neutrino flavor transformation. The CC and ES reaction rates are consistent with the earlier results [2] and with the NC reaction rate under the hypothesis of flavor transformation. The total flux of ^{8}B neutrinos measured with the NC reaction is in agreement with the SSM prediction.

This research was supported by: Canada: NSERC, Industry Canada, NRC, Northern Ontario Heritage Fund Corporation, Inco, AECL, Ontario Power Generation; US: Dept. of Energy; UK: PPARC. We thank the SNO technical staff for their strong contributions.

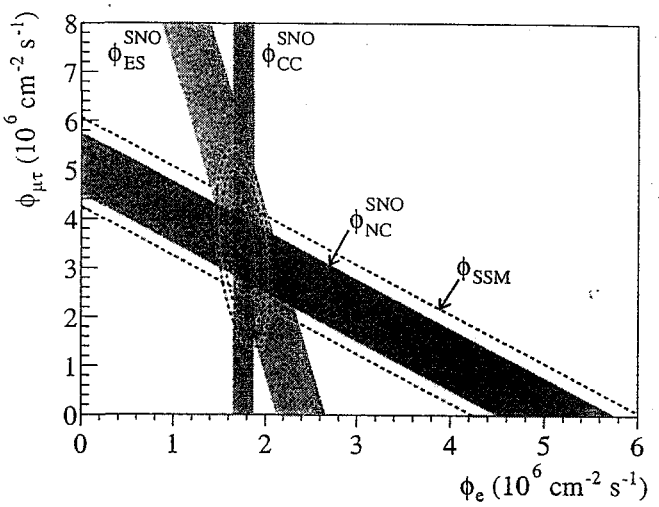

FIG. 3: Flux of ^{8}B solar neutrinos which are μ or τ flavor vs flux of electron neutrinos deduced from the three neutrino reactions in SNO. The diagonal bands show the total ^{8}B flux as predicted by the SSM [11] (dashed lines) and that measured with the NC reaction in SNO (solid band). The intercepts of these bands with the axes represent the $\pm 1\sigma$ errors. The bands intersect at the fit values for ϕ_e and $\phi_{\mu\tau}$, indicating that the combined flux results are consistent with neutrino flavor transformation assuming no distortion in the ^{8}B neutrino energy spectrum.

* Permanent Address: Birkbeck College, University of London, Malet Road, London WC1E 7HX, UK
† Deceased

[1] H. Chen, Phys. Rev. Lett. **55**, 1534 (1985).
[2] Q.R. Ahmad *et al.*, Phys. Rev. Lett. **87**, 071301 (2001).
[3] The SNO collaboration, Nucl. Instr. and Meth. **A449**, 172 (2000).
[4] M. R. Dragowsky *et al.*, Nucl. Instr. and Meth. **A481**, 284 (2002).
[5] M.-Q. Liu, H.W. Lee, and A.B. McDonald, Nucl. Inst. Meth. **A329**, 291 (1993).
[6] C. E. Ortiz *et al.*, Phys. Rev. Lett. **85**, 2909 (2000).
[7] Cross section uncertainty includes g_A uncertainty (0.6%), difference between NSGK (S. Nakamura, T. Sato, V. Gudkov and K. Kubodera, Phys. Rev. **C63** (2001) 034617) and BCK (M. Butler, J.-W. Chen and X. Kong, Phys. Rev. **C63** (2001) 035501) in SNO's calculations (0.6%), radiative correction uncertainties (0.3% for CC, 0.1% for NC, A. Kurylov, M. J. Ramsey-Musolf and P. Vogel, Phys. Rev. **C65** (2002) 055501), uncertainty associated with neglect of real photons in SNO (0.7% for CC), and theoretical cross section uncertainty (1%, S. Nakamura *et al.*, arXiv:nucl-th/0201062, (to be published)).
[8] Z. Maki, N. Nakagawa, and S. Sakata, Prog. Theor. Phys. **28**, 870 (1962).
[9] V. Gribov and B. Pontecorvo, Phys. Lett. **B28**, 493 (1969).
[10] S. Fukuda *et al.*, Phys. Rev. Lett. **86**, 5651 (2001).
[11] John N. Bahcall, M.H. Pinsonneault, and Sarbani Basu, Astrophys. J. **555**, 990 (2001).
[12] We note that this rate of neutron events also leads to a lower bound on the proton lifetime for "invisible" modes (based on the free neutron that would be left in deuterium (V.I. Tretyak and Yu.G. Zdesenko, Phys. Lett. **B505**, 59 (2001)) in excess of 10^{28} years, approximately

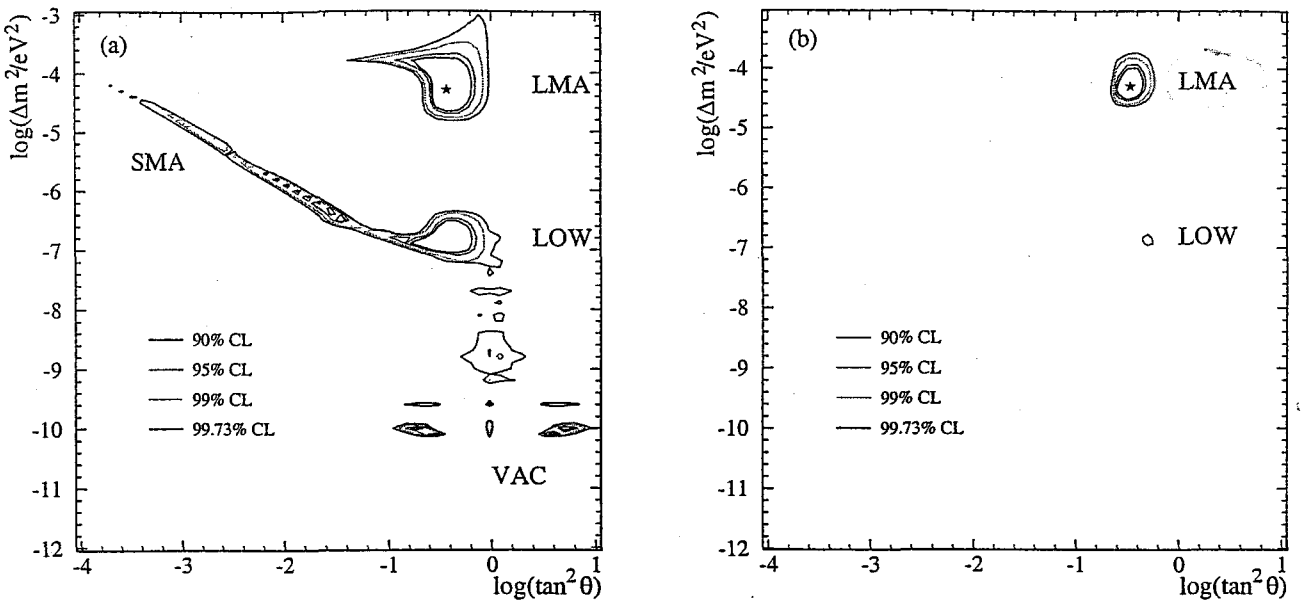

FIG. 4: Allowed regions of the MSW plane determined by a χ^2 fit to (a) SNO day and night energy spectra and (b) with additional experimental and solar model data. The star indicates the best fit. See text for details.

J. Tran Thanh Van (1986), vol. Editions Frontières, Gif-sur-Yvette, 1986, p. 335.

[4] A. J. Baltz and J. Weneser, Phys. Rev. D **37**, 3364 (1988).

[5] M. C. Gonzalez-Garcia, C. Peña-Garay and A. Y. Smirnov, Phys. Rev. D **63**, 113004 (2001).

[6] A non-zero value for $\mathcal{A}_{NC}$ might be evidence for sterile neutrinos.

[7] The SNO Collaboration, Nucl. Instr. and Meth. **A449**, 172 (2000).

[8] Details of SNO response functions are available from the SNO web site: http://sno.phy.queensu.ca

[9] M. Dragowsky *et al.*, Nucl. Instr. and Meth. **A481**, 284 (2002).

[10] S. Fukuda *et al.*, Phys. Rev. Lett. **86**, 5651 (2001).

[11] J. N. Bahcall, P. Krastev, and A. Y. Smirnov, Phys. Rev. D **62**, 093004 (2000); M. Maris and S. T. Petcov, Phys. Rev. D **62**, 093006 (2000); J. N. Bahcall, M. C. Gonzalez-Garcia, and C. Peña-Garay, (2002), hep-ph/0111150 v2.

[12] S. J. Parke, Phys. Rev. Lett. **57**, 1275 (1986); S. T. Petcov, Phys. Rev. B **200**, 373 (1988); G. L. Fogli and E. Lisi, Astropart. Phys. **3**, 185 (1995); E. Lisi, A. Marrone, D. Montanino, A. Palazzo, and S. T. Petcov, Phys. Rev. D **63**, 093002 (2001).

[13] C. E. Ortiz *et al.*, Phys. Rev. Lett. **85**, 2909 (2000).

[14] S. Nakamura *et al.* (2002), nucl-th/0201062.

[15] J. N. Bahcall, H. M. Pinsonneault and S. Basu, Astrophys. J **555**, 990 (2001).

[16] B. T. Cleveland *et al.*, Astrophys. J **496**, 505 (1998).

[17] J. N. Abdurashitov *et al.*, Phys. Rev. C **60**, 055801 (1999).

[18] J. N. Abdurashitov *et al.* (2002), astro-ph/0204245

[19] M. Altmann *et al.*, Phys. Lett. B **490**, 16 (2000).

[20] W. Hampel *et al.*, Phys. Lett. B **447**, 127 (1999).

[21] C. M. Cattadori *et al.*, in *Proceedings of the TAUP 2001 Workshop*, (September 2001), Assergi, Italy.

First Results from KamLAND: Evidence for Reactor Anti-Neutrino Disappearance

K. Eguchi,[1] S. Enomoto,[1] K. Furuno,[1] J. Goldman,[1] H. Hanada,[1] H. Ikeda,[1] K. Ikeda,[1] K. Inoue,[1] K. Ishihara,[1] W. Itoh,[1] T. Iwamoto,[1] T. Kawaguchi,[1] T. Kawashima,[1] H. Kinoshita,[1] Y. Kishimoto,[1] M. Koga,[1] Y. Koseki,[1] T. Maeda,[1] T. Mitsui,[1] M. Motoki,[1] K. Nakajima,[1] M. Nakajima,[1] T. Nakajima,[1] H. Ogawa,[1] K. Owada,[1] T. Sakabe,[1] I. Shimizu,[1] J. Shirai,[1] F. Suekane,[1] A. Suzuki,[1] K. Tada,[1] O. Tajima,[1] T. Takayama,[1] K. Tamae,[1] H. Watanabe,[1] J. Busenitz,[2] Ž. Djurčić,[2] K. McKinny,[2] D-M. Mei,[2] A. Piepke,[2] E. Yakushev,[2] B.E. Berger,[3] Y.D. Chan,[3] M.P. Decowski,[3] D.A. Dwyer,[3] S.J. Freedman,[3] Y. Fu,[3] B.K. Fujikawa,[3] K.M. Heeger,[3] K.T. Lesko,[3] K.-B. Luk,[3] H. Murayama,[3] D.R. Nygren,[3] C.E. Okada,[3] A.W.P. Poon,[3] H.M. Steiner,[3] L.A. Winslow,[3] G.A. Horton-Smith,[4] R.D. McKeown,[4] J. Ritter,[4] B. Tipton,[4] P. Vogel,[4] C.E. Lane,[5] T. Miletic,[5] P.W. Gorham,[6] G. Guillian,[6] J.G. Learned,[6] J. Maricic,[6] S. Matsuno,[6] S. Pakvasa,[6] S. Dazeley,[7] S. Hatakeyama,[7] M. Murakami,[7] R.C. Svoboda,[7] B.D. Dieterle,[8] M. DiMauro,[8] J. Detwiler,[9] G. Gratta,[9] K. Ishii,[9] N. Tolich,[9] Y. Uchida,[9] M. Batygov,[10] W. Bugg,[10] H. Cohn,[10] Y. Efremenko,[10] Y. Kamyshkov,[10] A. Kozlov,[10] Y. Nakamura,[10] L. De Braeckeleer,[11] C.R. Gould,[11] H.J. Karwowski,[11] D.M. Markoff,[11] J.A. Messimore,[11] K. Nakamura,[11] R.M. Rohm,[11] W. Tornow,[11] A.R. Young,[11] and Y-F. Wang[12]

(KamLAND Collaboration)

[1] *Research Center for Neutrino Science, Tohoku University, Sendai 980-8578, Japan*
[2] *Department of Physics and Astronomy, University of Alabama, Tuscaloosa, Alabama 35487, USA*
[3] *Physics Department, University of California at Berkeley and Lawrence Berkeley National Laboratory, Berkeley, California 94720, USA*
[4] *W. K. Kellogg Radiation Laboratory, California Institute of Technology, Pasadena, California 91125, USA*
[5] *Physics Department, Drexel University, Philadelphia, Pennsylvania 19104, USA*
[6] *Department of Physics and Astronomy, University of Hawaii at Manoa, Honolulu, Hawaii 96822, USA*
[7] *Department of Physics and Astronomy, Louisiana State University, Baton Rouge, Louisiana 70803, USA*
[8] *Physics Department, University of New Mexico, Albuquerque, New Mexico 87131, USA*
[9] *Physics Department, Stanford University, Stanford, California 94305, USA*
[10] *Department of Physics and Astronomy, University of Tennessee, Knoxville, Tennessee 37996, USA*
[11] *Triangle Universities Nuclear Laboratory, Durham, North Carolina 27708, USA and Physics Departments at Duke University, North Carolina State University, and the University of North Carolina at Chapel Hill*
[12] *Institute of High Energy Physics, Beijing 100039, People's Republic of China*

(Dated: December 6, 2002)

KamLAND has been used to measure the flux of $\bar{\nu}_e$'s from distant nuclear reactors. In an exposure of 162 ton·yr (145.1 days) the ratio of the number of observed inverse β-decay events to the expected number of events without disappearance is $0.611 \pm 0.085(\text{stat}) \pm 0.041(\text{syst})$ for $\bar{\nu}_e$ energies > 3.4 MeV. The deficit of events is inconsistent with the expected rate for standard $\bar{\nu}_e$ propagation at the 99.95% confidence level. In the context of two-flavor neutrino oscillations with CPT invariance, these results exclude all oscillation solutions but the 'Large Mixing Angle' solution to the solar neutrino problem using reactor $\bar{\nu}_e$ sources.

PACS numbers: 14.60.Pq, 26.65.+t, 28.50.Hw, 91.65.Dt

The primary goal of the Kamioka Liquid scintillator Anti-Neutrino Detector (KamLAND) experiment [1] is a search for the oscillation of $\bar{\nu}_e$'s emitted from distant power reactors. The long baseline, typically 180 km, enables KamLAND to address the oscillation solution of the 'solar neutrino problem' using reactor anti-neutrinos under laboratory conditions. The inverse β-decay reaction, $\bar{\nu}_e + p \rightarrow e^+ + n$, is utilized to detect $\bar{\nu}_e$'s with energies above 1.8 MeV in liquid scintillator (LS) [2]. The detection of the e^+ and the 2.2 MeV γ-ray from neutron capture on a proton in delayed coincidence is a powerful tool for reducing background. This letter presents the first results from an analysis of 162 ton·yr of the reactor $\bar{\nu}_e$ data.

KamLAND is located at the site of the earlier Kamiokande [3], with an average rock overburden of 2,700 m.w.e. resulting in 0.34 Hz of cosmic-ray muons in the detector volume. As shown in Fig. 1, the neutrino detector/target is 1 kton of ultra-pure LS contained in a 13-m-diameter spherical balloon made of 135-μm-thick transparent nylon/EVOH (Ethylene vinyl alcohol copolymer) composite film. The balloon is supported and constrained by a network of kevlar ropes. The LS is 80% dodecane, 20% pseudocumene (1,2,4-Trimethylbenzene), and 1.52 g/liter of PPO (2,5-Diphenyloxazole) as a fluor. A buffer of dodecane and isoparaffin oils between the balloon and an 18-m-diameter spherical stainless-steel containment vessel shields the LS from external radiation. During the filling procedure a water extraction and nitrogen bubbling method [4], optimized for KamLAND, was used to purify the LS and buffer oil; PPO prepurification was especially important.

KAMLAND: REACTOR $\bar{\nu}_e$

$\bar{E} \sim 2$ MeV

16 REACTORS $\bar{L} \sim 180$ km

TEST OF THE MSW LMA SOLUTION.

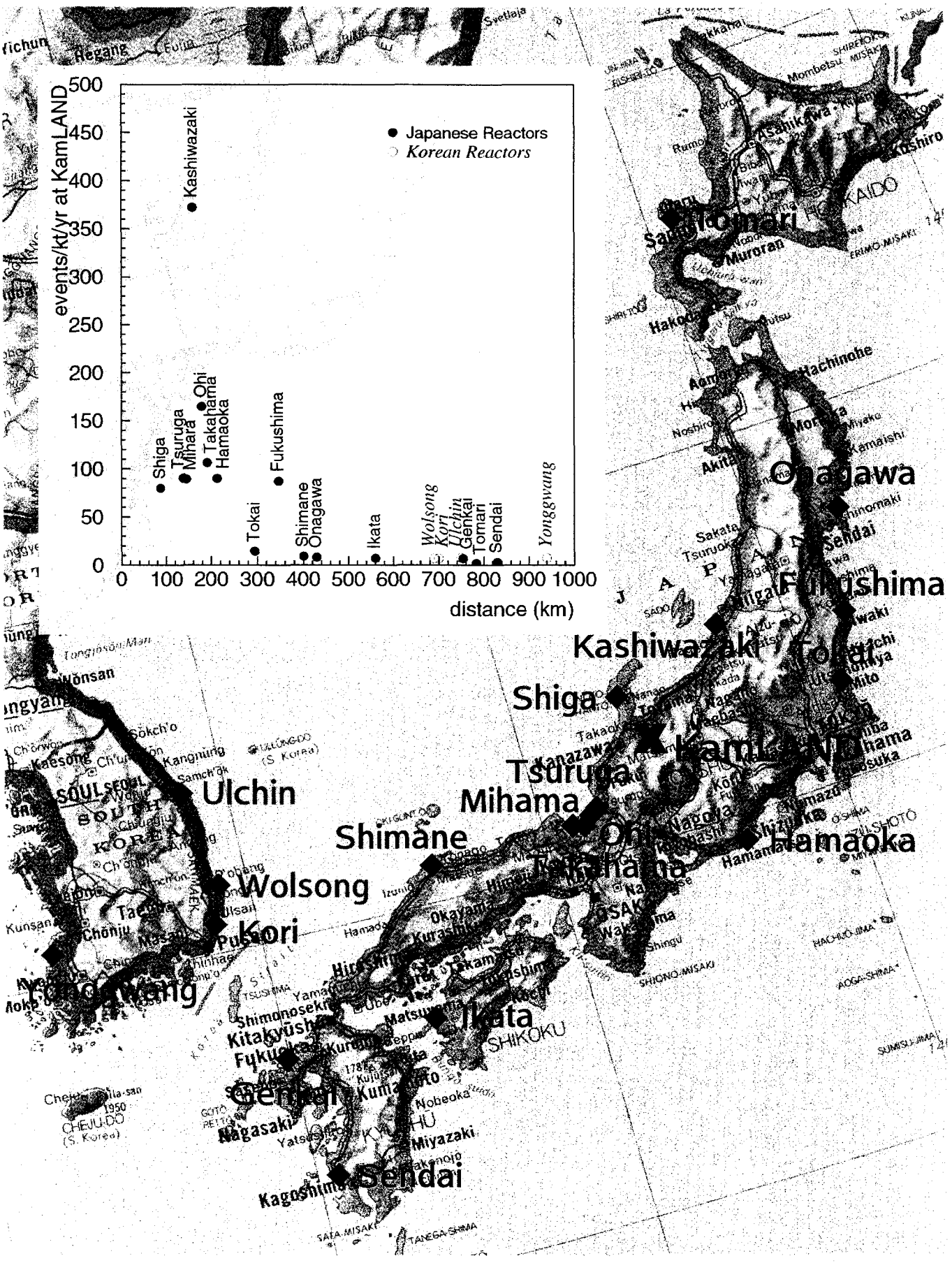
events/kt/yr at KamLAND
distance (km)
Japanese Reactors
Korean Reactors
Kashiwazaki
Shiga
Tsuruga
Mihama
Ohi
Takahama
Hamaoka
Fukushima
Tokai
Shimane
Onagawa
Ikata
Wolsong
Kori
Ulchin
Genkai
Tomari
Sendai
Yonggwang
Kashiwazaki
Shiga
Tsuruga
Mihama
Shimane
Hamaoka
Fukushima
Onagawa
Tomari
Ulchin
Wolsong
Kori
Ikata
Genkai
Sendai
KamLAND

Contribution of each reactors

Reactor	(km)	(ev/kt/yr)	
Shiga	88	80.0	
Tsuruga	138	90.7	
Fugen	138	10.0	
Mihama	146	89.4	
Kashiwazaki	160	372.4	79%
Ohi	179	164.8	
Takahama	192	106.4	
Hamaoka	214	90.2	
Tokai	295	14.6	
Fukushima2	345	42.8	
Fukushima1	349	44.6	
Shimane	401	9.2	
Onagawa	431	8.4	
Ikata	561	7.3	
Genkai	755	7.0	
Tomari	783	2.0	
Sendai	830	3.0	
Wolsong	709	6.2	
Ulchin	712	8.6	2.4%
Kori	735	6.3	
Yonggwang	987	6.7	

Sum Rate (Max Power) 1171 ⇨ 1113 (−5%)

$^{235}U/^{239}Pu/^{238}U/^{241}Pu$ = 60.5/27.2/7.7/4.6 ⇨ 45.0/38.8/8.3/7.9

$$P(\bar{\nu}_e \rightarrow \bar{\nu}_e) = 1 - \frac{1}{2}\sin^2 2\theta_\odot \left[1 - \cos\frac{\Delta m^2_\odot}{2E} L\right]$$

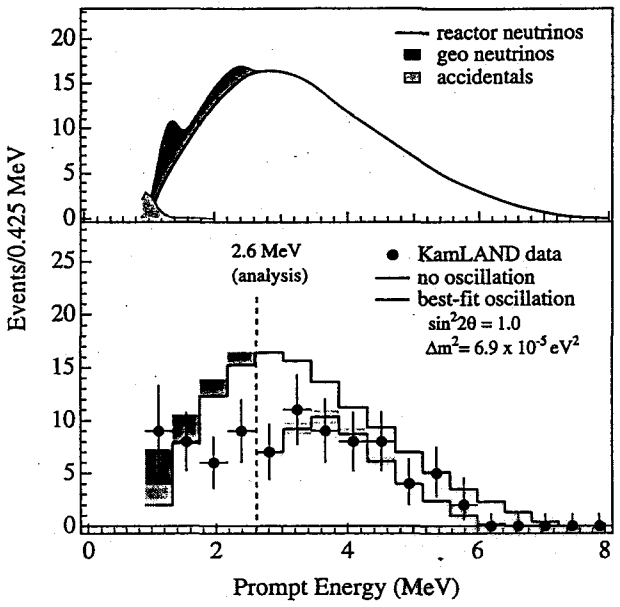

FIG. 5: Upper panel: Expected reactor $\bar{\nu}_e$ energy spectrum with contributions of $\bar{\nu}_{geo}$ (model Ia of [6]) and accidental backround. Lower panel: Energy spectrum of the observed prompt events (solid circles with error bars), along with the expected no oscillation spectrum (upper histogram, with $\bar{\nu}_{geo}$ and accidentals shown) and best fit (lower histogram) including neutrino oscillations. The shaded band indicates the systematic error in the best-fit spectrum. The vertical dashed line corresponds to the analysis threshold at 2.6 MeV.

the present sample before the energy cuts are applied is shown in Fig. 3. A clear cluster of events from the 2.2 MeV capture γ's is observed. One event with delayed energy around 5 MeV is consistent with a thermal neutron capture γ on ^{12}C. The space-time correlation of the prompt and delayed events is in good agreement with expectations, and the observed mean neutron capture time is 188 ± 23 μsec. After applying the prompt and delayed energy cuts, 54 events remain as the final sample. The ratio of the number of observed reactor $\bar{\nu}_e$ events to that expected in the absence of neutrino oscillations is

$$\frac{N_{obs} - N_{BG}}{N_{expected}} = 0.611 \pm 0.085(\text{stat}) \pm 0.041(\text{syst}).$$

The probability that the KamLAND result is consistent with the no disappearance hypothesis is less than 0.05%. Fig. 4 shows the ratio of measured to expected flux for KamLAND as well as previous reactor experiments as a function of the average distance from the source.

The observed prompt energy spectrum is shown in Fig. 5. The expected positron spectrum with no oscillations and the best fit with two-flavor neutrino oscillations above the 2.6 MeV threshold are shown. A clear deficit of events is observed. The measured spectrum is consistent (93% confidence) with a distorted spectrum shape as expected from neutrino oscillations, but a renormalized no-oscillation shape is also consistent at 53% confidence.

The neutrino oscillation parameter region for two-neutrino mixing is shown in Fig. 6. The dark shaded area is the LMA region at 95% C.L. derived from [13]. The shaded region outside the solid line is excluded at 95% C.L. from the rate analysis with

$$\chi^2 = \frac{(0.611 - R(\sin^2 2\theta, \Delta m^2))^2}{0.085^2 + 0.041^2}.$$

Here, $R(\sin^2 2\theta, \Delta m^2)$ is the expected ratio with the oscillation parameters.

The spectrum of the final event sample is then analyzed with a maximum likelihood method to obtain the optimum set of oscillation parameters with the following χ^2 definition:

$$\begin{aligned}\chi^2 &= \chi^2_{\text{rate}}(\sin^2 2\theta, \Delta m^2, N_{\text{BG1}\sim 2}, \alpha_{1\sim 4}) \\ &\quad -2\log L_{\text{shape}}(\sin^2 2\theta, \Delta m^2, N_{\text{BG1}\sim 2}, \alpha_{1\sim 4}) \\ &\quad +\chi^2_{\text{BG}}(N_{\text{BG1}\sim 2}) + \chi^2_{\text{distortion}}(\alpha_{1\sim 4}),\end{aligned}$$

where L_{shape} is the likelihood function of the spectrum including deformations from various parameters. $N_{\text{BG1}\sim 2}$ are the number of ^{9}Li and ^{8}He backgrounds and $\alpha_{1\sim 4}$ are the parameters for the shape deformation coming from energy scale, resolution, $\bar{\nu}_e$ spectrum and fiducial volume. These parameters are varied to minimize the χ^2 at each pair of oscillation parameters with a bound from $\chi^2_{\text{BG}}(N_{\text{BG1}\sim 2})$ and $\chi^2_{\text{distortion}}(\alpha_{1\sim 4})$. The best fit to the KamLAND data in the physical region yields $\sin^2 2\theta = 1.0$ and $\Delta m^2 = 6.9 \times 10^{-5}$ eV^2 while the global minimum occurs slightly outside of the physical region at $\sin^2 2\theta = 1.01$ with the same Δm^2. These numbers can be compared to the best fit LMA values of $\sin^2 2\theta = 0.833$ and $\Delta m^2 = 5.5 \times 10^{-5}$ eV^2 from [13]. The 95% C.L. allowed regions from the spectrum shape analysis are shown in Fig. 6. The allowed regions displayed for KamLAND correspond to $0 < \theta < \frac{\pi}{4}$ consistent with the solar LMA solution, but for KamLAND the allowed regions in $\frac{\pi}{4} < \theta < \frac{\pi}{2}$ are identical [14].

Another spectrum shape analysis is performed with a lower prompt energy threshold of 0.9 MeV in order to check the stability of the above result and study the sensitivity to $\bar{\nu}_{geo}$. With this threshold, the total background is estimated to be 2.91 ± 1.12 events, most of which come from accidental and spallation events. The systematic error is 6.0%, which is smaller than that for the final event sample due to the absence of an energy threshold effect. When the maximum likelihood is calculated, the $\bar{\nu}_{geo}$ fluxes from ^{238}U and ^{232}Th are treated as free parameters. The best fit in this analysis yields $\sin^2 2\theta = 0.91$ and $\Delta m^2 = 6.9 \times 10^{-5}$eV^2. These results and the allowed region of the oscillation parameters are in good agreement with the results obtained above. The numbers of $\bar{\nu}_{geo}$ events for the best fit are 4 for ^{238}U and 5 for ^{232}Th, which corresponds to $\sim$40 TW radiogenic heat generation according to model Ia in [6]. However, for the same model $\bar{\nu}_{geo}$ production powers from 0 to 110 TW

Measurement of the Total Active ^{8}B Solar Neutrino Flux at the Sudbury Neutrino Observatory with Enhanced Neutral Current Sensitivity

S.N. Ahmed,[10] A.E. Anthony,[14] E.W. Beier,[9] A. Bellerive,[3] S.D. Biller,[8] J. Boger,[2] M.G. Boulay,[7] M.G. Bowler,[8] T.J. Bowles,[7] S.J. Brice,[7] T.V. Bullard,[13] Y.D. Chan,[6] M. Chen,[10] X. Chen,[6] B.T. Cleveland,[8] G.A. Cox,[13] X. Dai,[3,8] F. Dalnoki-Veress,[3] P.J. Doe,[13] R.S. Dosanjh,[3] G. Doucas,[8] M.R. Dragowsky,[7] C.A. Duba,[13] F.A. Duncan,[10] M. Dunford,[9] J.A. Dunmore,[8] E.D. Earle,[10] S.R. Elliott,[7] H.C. Evans,[10] G.T. Ewan,[10] J. Farine,[5,3] H. Fergani,[8] F. Fleurot,[5] J.A. Formaggio,[13] M.M. Fowler,[7] K. Frame,[8,3] B.G. Fulsom,[10] N. Gagnon,[13,7,6,8] K. Graham,[10] D.R. Grant,[3] R.L. Hahn,[2] J.C. Hall,[14] A.L. Hallin,[10] E.D. Hallman,[5] A.S. Hamer,[7,*] W.B. Handler,[10] C.K. Hargrove,[3] P.J. Harvey,[10] R. Hazama,[13] K.M. Heeger,[6] W.J. Heintzelman,[9] J. Heise,[7] R.L. Helmer,[12,1] R.J. Hemingway,[3] A. Hime,[7] M.A. Howe,[13] P. Jagam,[4] N.A. Jelley,[8] J.R. Klein,[14,9] M.S. Kos,[10] A.V. Krumins,[10] T. Kutter,[1] C.C.M. Kyba,[9] H. Labranche,[4] R. Lange,[2] J. Law,[4] I.T. Lawson,[4] K.T. Lesko,[6] J.R. Leslie,[10] I. Levine,[3,†] S. Luoma,[5] R. MacLellan,[10] S. Majerus,[8] H.B. Mak,[10] J. Maneira,[10] A.D. Marino,[6] N. McCauley,[9] A.B. McDonald,[10] S. McGee,[13] G. McGregor,[8] C. Mifflin,[3] K.K.S. Miknaitis,[13] G.G. Miller,[7] B.A. Moffat,[10] C.W. Nally,[1] B.G. Nickel,[4] A.J. Noble,[10,3,12] E.B. Norman,[6] N.S. Oblath,[13] C.E. Okada,[6] R.W. Ollerhead,[4] J.L. Orrell,[13] S.M. Oser,[1,9] C. Ouellet,[10] S.J.M. Peeters,[8] A.W.P. Poon,[6] B.C. Robertson,[10] R.G.H. Robertson,[13] E. Rollin,[3] S.S.E. Rosendahl,[6] V.L. Rusu,[9] M.H. Schwendener,[5] O. Simard,[3] J.J. Simpson,[4] C.J. Sims,[8] D. Sinclair,[3,12] P. Skensved,[10] M.W.E. Smith,[13] N. Starinsky,[3] R.G. Stokstad,[6] L.C. Stonehill,[13] R. Tafirout,[5] Y. Takeuchi,[10] G. Tešić,[3] M. Thomson,[10] M. Thorman,[8] R. Van Berg,[9] R.G. Van de Water,[7] C.J. Virtue,[5] B.L. Wall,[13] D. Waller,[3] C.E. Waltham,[1] H. Wan Chan Tseung,[8] D.L. Wark,[11] N. West,[8] J.B. Wilhelmy,[7] J.F. Wilkerson,[13] J.R. Wilson,[8] J.M. Wouters,[7] M. Yeh,[2] and K. Zuber[8]

(SNO Collaboration)

[1] *Department of Physics and Astronomy, University of British Columbia, Vancouver, BC V6T 1Z1 Canada*
[2] *Chemistry Department, Brookhaven National Laboratory, Upton, NY 11973-5000*
[3] *Ottawa-Carleton Institute for Physics, Department of Physics, Carleton University, Ottawa, Ontario K1S 5B6 Canada*
[4] *Physics Department, University of Guelph, Guelph, Ontario N1G 2W1 Canada*
[5] *Department of Physics and Astronomy, Laurentian University, Sudbury, Ontario P3E 2C6 Canada*
[6] *Institute for Nuclear and Particle Astrophysics and Nuclear Science Division, Lawrence Berkeley National Laboratory, Berkeley, CA 94720*
[7] *Los Alamos National Laboratory, Los Alamos, NM 87545*
[8] *Department of Physics, University of Oxford, Denys Wilkinson Building, Keble Road, Oxford, OX1 3RH, UK*
[9] *Department of Physics and Astronomy, University of Pennsylvania, Philadelphia, PA 19104-6396*
[10] *Department of Physics, Queen's University, Kingston, Ontario K7L 3N6 Canada*
[11] *Rutherford Appleton Laboratory, Chilton, Didcot, Oxon, OX11 0QX, and University of Sussex, Physics and Astronomy Department, Brighton BN1 9QH, UK*
[12] *TRIUMF, 4004 Wesbrook Mall, Vancouver, BC V6T 2A3, Canada*
[13] *Center for Experimental Nuclear Physics and Astrophysics, and Department of Physics, University of Washington, Seattle, WA 98195*
[14] *Department of Physics, University of Texas at Austin, Austin, TX 78712-0264*

(Dated: 9 September 2003)

The Sudbury Neutrino Observatory (SNO) has precisely determined the total active (ν_x) ^{8}B solar neutrino flux without assumptions about the energy dependence of the ν_e survival probability. The measurements were made with dissolved NaCl in the heavy water to enhance the sensitivity and signature for neutral-current interactions. The flux is found to be 5.21 ± 0.27 (stat) ± 0.38 (syst) $\times 10^6$ cm^{-2}s^{-1}, in agreement with previous measurements and standard solar models. A global analysis of these and other solar and reactor neutrino results yields $\Delta m^2 = 7.1^{+1.2}_{-0.6} \times 10^{-5}$ eV^2 and $\theta = 32.5^{+2.4}_{-2.3}$ degrees. Maximal mixing is rejected at the equivalent of 5.4 standard deviations.

PACS numbers: 26.65.+t, 14.60.Pq, 13.15.+g, 95.85.Ry

The Sudbury Neutrino Observatory (SNO) [1] detects ^{8}B solar neutrinos through the reactions

$$\begin{aligned} \nu_e + d &\rightarrow p + p + e^- && \text{(CC)}, \\ \nu_x + d &\rightarrow p + n + \nu_x && \text{(NC)}, \\ \nu_x + e^- &\rightarrow \nu_x + e^- && \text{(ES)}. \end{aligned}$$

Only electron neutrinos produce charged-current interactions (CC), while the neutral-current (NC) and elastic scattering (ES) reactions have sensitivity to non-electron flavors. The NC reaction measures the total flux of all active neutrino flavors above a threshold of 2.2 MeV.

SNO previously measured the NC rate by observing neutron captures on deuterons, and found that a Standard-Model description with an undistorted ^{8}B neutrino spectrum and CC, ES, and NC rates due solely to ν_e interactions was rejected [2, 3]. This Letter presents measurements of the CC, NC, and ES rates from SNO's dissolved salt phase.

The addition of 2 tonnes of NaCl to the kilotonne of heavy water increased the neutron capture efficiency and the associated Cherenkov light. The solution was thoroughly mixed and

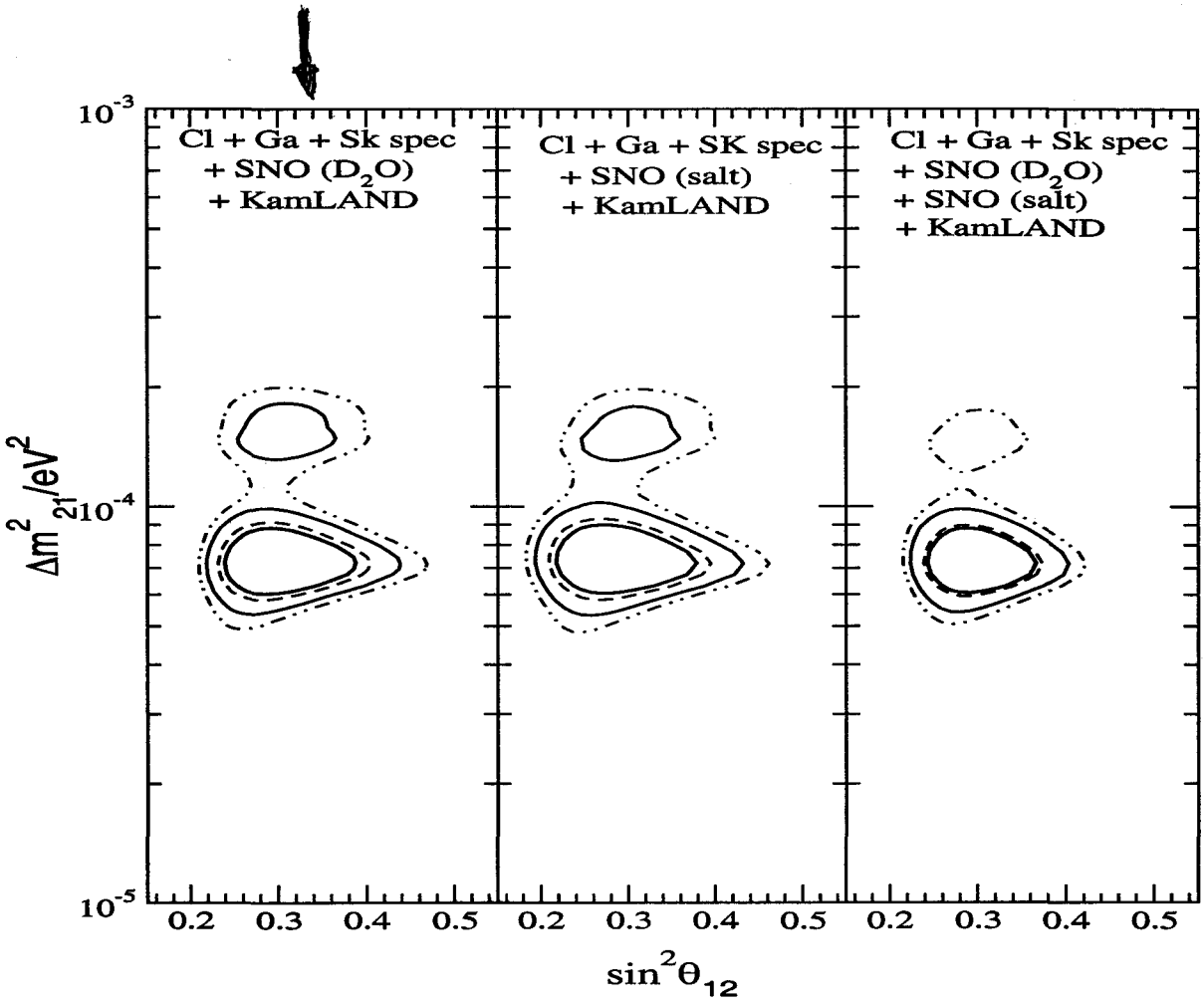

$$\Delta m^2_{\odot} \equiv \Delta m^2_{21} = 7.2 \times 10^{-5}\ \text{eV}^2\ ,$$

$$\sin^2\theta_{\odot} \equiv \sin^2\theta_{12} = 0.30\ ;$$

$$\cos 2\theta_{12} = 0.40; \quad \cos 2\theta_{12} > 0.20, \quad 99\%\ \text{C.L.}$$

- $\sin^2\theta_{12} = 0.50$ excluded at > 5 s.d.
- Low-LMA statistically favored
- High-LMA allowed only at $\sim 99.15\%$ C.L.

A. Bandyopadhyay et al, hep-ph/0309174

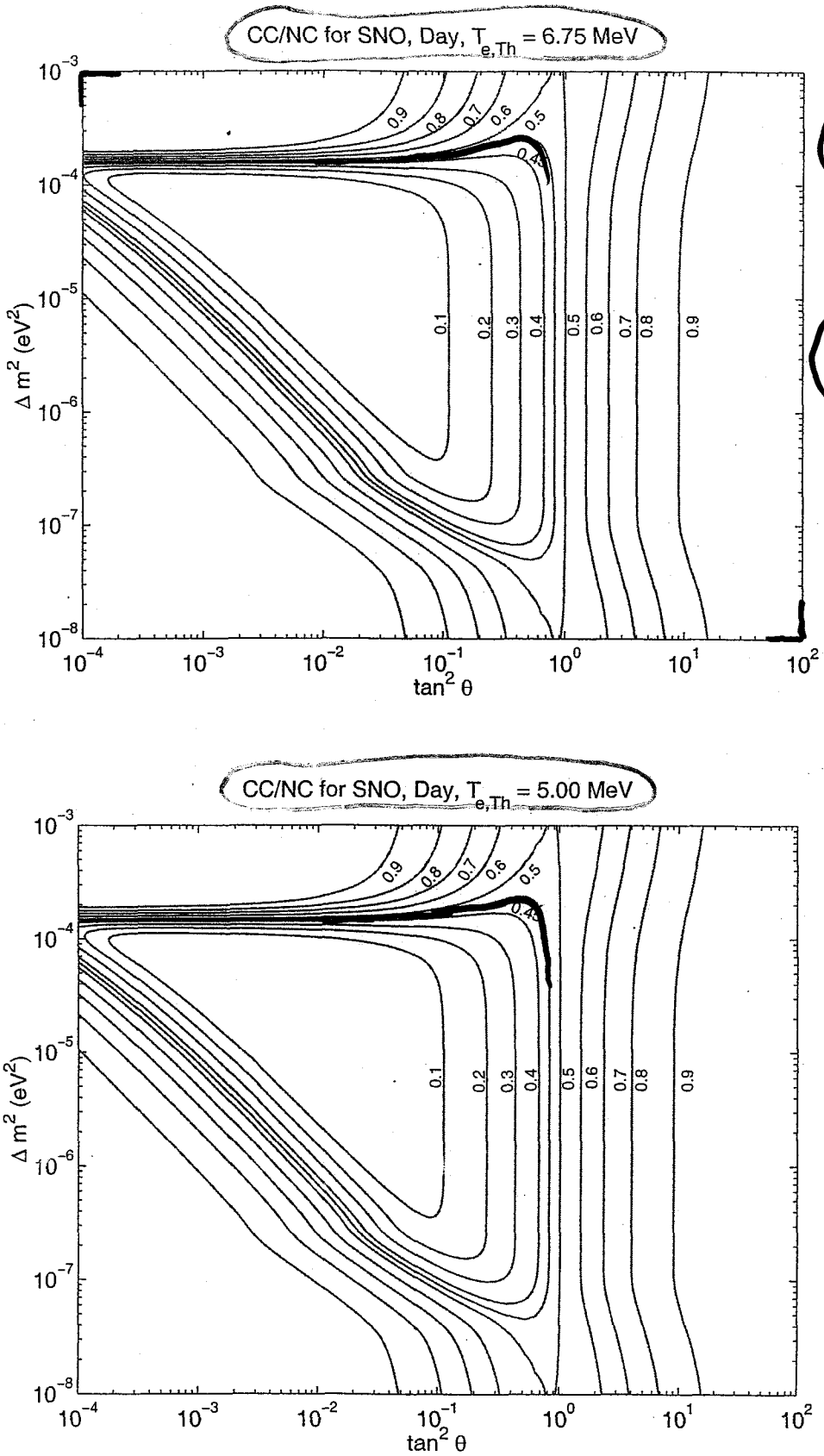

Figure 4: Iso$-R^{SNO}_{CC/NC}(D)$ contour plots for $T_{\rm e,th} = 6.75$ MeV (upper panel) and $T_{\rm e,th} = 5.00$ MeV (lower panel): each contour corresponds to a fixed value of the *Day* ratio of the CC and NC solar neutrino event rates measured in the SNO experiment. In the case of absence of oscillations of solar neutrinos $R^{SNO}_{CC/NC}(D) = 1$. The contours shown are for $R^{SNO}_{CC/NC}(D) = 0.10$, 0.20, 0.30, 0.40, 0.45, 0.50, 0.60, 0.70, 0.80, 0.90.

Measurement of the Total Active ^{8}B Solar Neutrino Flux at the Sudbury Neutrino Observatory with Enhanced Neutral Current Sensitivity

S.N. Ahmed,[10] A.E. Anthony,[14] E.W. Beier,[9] A. Bellerive,[3] S.D. Biller,[8] J. Boger,[2] M.G. Boulay,[7] M.G. Bowler,[8] T.J. Bowles,[7] S.J. Brice,[7] T.V. Bullard,[13] Y.D. Chan,[6] M. Chen,[10] X. Chen,[6] B.T. Cleveland,[8] G.A. Cox,[13] X. Dai,[3,8] F. Dalnoki-Veress,[3] P.J. Doe,[13] R.S. Dosanjh,[3] G. Doucas,[8] M.R. Dragowsky,[7] C.A. Duba,[13] F.A. Duncan,[10] M. Dunford,[9] J.A. Dunmore,[8] E.D. Earle,[10] S.R. Elliott,[7] H.C. Evans,[10] G.T. Ewan,[10] J. Farine,[5,3] H. Fergani,[8] F. Fleurot,[5] J.A. Formaggio,[13] M.M. Fowler,[7] K. Frame,[8,3] B.G. Fulsom,[10] N. Gagnon,[13,7,6,8] K. Graham,[10] D.R. Grant,[3] R.L. Hahn,[2] J.C. Hall,[14] A.L. Hallin,[10] E.D. Hallman,[5] A.S. Hamer,[7,*] W.B. Handler,[10] C.K. Hargrove,[3] P.J. Harvey,[10] R. Hazama,[13] K.M. Heeger,[6] W.J. Heintzelman,[9] J. Heise,[7] R.L. Helmer,[12,1] R.J. Hemingway,[3] A. Hime,[7] M.A. Howe,[13] P. Jagam,[4] N.A. Jelley,[8] J.R. Klein,[14,9] M.S. Kos,[10] A.V. Krumins,[10] T. Kutter,[1] C.C.M. Kyba,[9] H. Labranche,[4] R. Lange,[2] J. Law,[4] I.T. Lawson,[4] K.T. Lesko,[6] J.R. Leslie,[10] I. Levine,[3,†] S. Luoma,[5] R. MacLellan,[10] S. Majerus,[8] H.B. Mak,[10] J. Maneira,[10] A.D. Marino,[6] N. McCauley,[9] A.B. McDonald,[10] S. McGee,[13] G. McGregor,[8] C. Mifflin,[3] K.K.S. Miknaitis,[13] G.G. Miller,[7] B.A. Moffat,[10] C.W. Nally,[1] B.G. Nickel,[4] A.J. Noble,[10,3,12] E.B. Norman,[6] N.S. Oblath,[13] C.E. Okada,[6] R.W. Ollerhead,[4] J.L. Orrell,[13] S.M. Oser,[1,9] C. Ouellet,[10] S.J.M. Peeters,[8] A.W.P. Poon,[6] B.C. Robertson,[10] R.G.H. Robertson,[13] E. Rollin,[3] S.S.E. Rosendahl,[6] V.L. Rusu,[9] M.H. Schwendener,[5] O. Simard,[3] J.J. Simpson,[4] C.J. Sims,[8] D. Sinclair,[3,12] P. Skensved,[10] M.W.E. Smith,[13] N. Starinsky,[3] R.G. Stokstad,[6] L.C. Stonehill,[13] R. Tafirout,[5] Y. Takeuchi,[10] G. Tešić,[3] M. Thomson,[10] M. Thorman,[8] R. Van Berg,[9] R.G. Van de Water,[7] C.J. Virtue,[5] B.L. Wall,[13] D. Waller,[3] C.E. Waltham,[1] H. Wan Chan Tseung,[8] D.L. Wark,[11] N. West,[8] J.B. Wilhelmy,[7] J.F. Wilkerson,[13] J.R. Wilson,[8] J.M. Wouters,[7] M. Yeh,[2] and K. Zuber[8]

(SNO Collaboration)

[1] *Department of Physics and Astronomy, University of British Columbia, Vancouver, BC V6T 1Z1 Canada*
[2] *Chemistry Department, Brookhaven National Laboratory, Upton, NY 11973-5000*
[3] *Ottawa-Carleton Institute for Physics, Department of Physics, Carleton University, Ottawa, Ontario K1S 5B6 Canada*
[4] *Physics Department, University of Guelph, Guelph, Ontario N1G 2W1 Canada*
[5] *Department of Physics and Astronomy, Laurentian University, Sudbury, Ontario P3E 2C6 Canada*
[6] *Institute for Nuclear and Particle Astrophysics and Nuclear Science Division, Lawrence Berkeley National Laboratory, Berkeley, CA 94720*
[7] *Los Alamos National Laboratory, Los Alamos, NM 87545*
[8] *Department of Physics, University of Oxford, Denys Wilkinson Building, Keble Road, Oxford, OX1 3RH, UK*
[9] *Department of Physics and Astronomy, University of Pennsylvania, Philadelphia, PA 19104-6396*
[10] *Department of Physics, Queen's University, Kingston, Ontario K7L 3N6 Canada*
[11] *Rutherford Appleton Laboratory, Chilton, Didcot, Oxon, OX11 0QX, and University of Sussex, Physics and Astronomy Department, Brighton BN1 9QH, UK*
[12] *TRIUMF, 4004 Wesbrook Mall, Vancouver, BC V6T 2A3, Canada*
[13] *Center for Experimental Nuclear Physics and Astrophysics, and Department of Physics, University of Washington, Seattle, WA 98195*
[14] *Department of Physics, University of Texas at Austin, Austin, TX 78712-0264*

(Dated: 9 September 2003)

The Sudbury Neutrino Observatory (SNO) has precisely determined the total active (ν_x) ^{8}B solar neutrino flux without assumptions about the energy dependence of the ν_e survival probability. The measurements were made with dissolved NaCl in the heavy water to enhance the sensitivity and signature for neutral-current interactions. The flux is found to be 5.21 ± 0.27 (stat) ± 0.38 (syst) $\times 10^6$ cm^{-2}s^{-1}, in agreement with previous measurements and standard solar models. A global analysis of these and other solar and reactor neutrino results yields $\Delta m^2 = 7.1^{+1.2}_{-0.6} \times 10^{-5}$ eV^2 and $\theta = 32.5^{+2.4}_{-2.3}$ degrees. Maximal mixing is rejected at the equivalent of 5.4 standard deviations.

PACS numbers: 26.65.+t, 14.60.Pq, 13.15.+g, 95.85.Ry

The Sudbury Neutrino Observatory (SNO) [1] detects ^{8}B solar neutrinos through the reactions

$$\begin{aligned} \nu_e + d &\rightarrow p + p + e^- && \text{(CC)}, \\ \nu_x + d &\rightarrow p + n + \nu_x && \text{(NC)}, \\ \nu_x + e^- &\rightarrow \nu_x + e^- && \text{(ES)}. \end{aligned}$$

Only electron neutrinos produce charged-current interactions (CC), while the neutral-current (NC) and elastic scattering (ES) reactions have sensitivity to non-electron flavors. The NC reaction measures the total flux of all active neutrino flavors above a threshold of 2.2 MeV.

SNO previously measured the NC rate by observing neutron captures on deuterons, and found that a Standard-Model description with an undistorted ^{8}B neutrino spectrum and CC, ES, and NC rates due solely to ν_e interactions was rejected [2, 3]. This Letter presents measurements of the CC, NC, and ES rates from SNO's dissolved salt phase.

The addition of 2 tonnes of NaCl to the kilotonne of heavy water increased the neutron capture efficiency and the associated Cherenkov light. The solution was thoroughly mixed and

TABLE I: Background events. The internal neutron and γ-ray backgrounds are constrained in the analysis. The external-source neutrons are reported from the fit. The last two Table entries are included in the systematic uncertainty estimates.

Source	Events
Deuteron photodisintegration	$73.1^{+24.0}_{-23.5}$
^{2}H(α,α)pn	2.8 ± 0.7
^{17,18}O(α,n)	1.4 ± 0.9
Fission, atmospheric ν (NC + sub-Cherenkov threshold CC)	23.0 ± 7.2
Terrestrial and reactor $\bar{\nu}$'s	2.3 ± 0.8
Neutrons from rock	≤ 1
^{24}Na activation	8.4 ± 2.3
n from CNO ν's	0.3 ± 0.3
Total internal neutron background	$111.3^{+25.3}_{-24.9}$
Internal γ (fission, atmospheric ν)	5.2 ± 1.3
^{16}N decays	< 2.5 (68% CL)
External-source neutrons (from fit)	$84.5^{+34.5}_{-33.6}$
Cherenkov events from $\beta - \gamma$ decays	< 14.7 (68% CL)
"AV events"	< 5.4 (68% CL)

TABLE II: Systematic uncertainties on fluxes for the spectral shape unconstrained analysis of the salt data set. † denotes CC vs NC anti-correlation.

Source	NC uncert. (%)	CC uncert. (%)	ES uncert. (%)
Energy scale	-3.7,+3.6	-1.0,+1.1	±1.8
Energy resolution	±1.2	±0.1	±0.3
Energy non-linearity	±0.0	-0.0,+0.1	±0.0
Radial accuracy	-3.0,+3.5	-2.6,+2.5	-2.6,+2.9
Vertex resolution	±0.2	±0.0	±0.2
Angular resolution	±0.2	±0.2	±2.4
Isotropy mean †	-3.4,+3.1	-3.4,+2.6	-0.9,+1.1
Isotropy resolution	±0.6	±0.4	±0.2
Radial energy bias	-2.4,+1.9	±0.7	-1.3,+1.2
Vertex Z accuracy †	-0.2,+0.3	±0.1	±0.1
Internal background neutrons	-1.9,+1.8	±0.0	±0.0
Internal background γ's	±0.1	±0.1	±0.0
Neutron capture	-2.5,+2.7	±0.0	±0.0
Cherenkov backgrounds	-1.1,+0.0	-1.1,+0.0	±0.0
"AV events"	-0.4,+0.0	-0.4,+0.0	±0.0
Total experimental uncertainty	-7.3,+7.2	-4.6,+3.8	-4.3,+4.5
Cross section [13]	±1.1	±1.2	±0.5

ual activation after calibrations and ^{24}Na production in the water circulation system and in the heavy water in the "neck" of the vessel were determined and are included in Table I. SNO is slightly sensitive to solar CNO neutrinos from the electron-capture decay of ^{15}O and ^{17}F.

Neutrons and γ rays produced at the acrylic vessel and in the light water can propagate into the fiducial volume. Radon progeny deposited on the surfaces of the vessel during construction can initiate (α,n) reactions on ^{13}C, ^{17}O, and ^{18}O, and external γ rays can photodisintegrate deuterium. The enhanced neutron capture efficiency of salt makes these external-source neutrons readily apparent, and an additional distribution function was included in the analysis to extract this component (Table I). Previous measurements [2, 3, 12] with pure D_2O were less sensitive to this background source, and a preliminary evaluation indicates the number of these background events was within the systematic uncertainties reported.

The backgrounds from Cherenkov events inside and outside the fiducial volume were estimated using calibration source data, measured activity, Monte Carlo calculations, and controlled injections of Rn into the detector. These backgrounds were nearly negligible above the analysis energy threshold and within the fiducial volume, and are included as an uncertainty on the flux measurements.

A class of background events identified and removed from the analysis in the pure D_2O phase ("AV events") reconstruct near the acrylic vessel and were characterized by a nearly isotropic light distribution. Analyses of the pure D_2O and salt data sets limit this background to 5.4 events (68% CL) for the present data.

To minimize the possibility of introducing biases, a blind analysis procedure was used. The data set used during the development of the analysis procedures and the definition of parameters excluded an unknown fraction (< 30%) of the final data set, included an unknown admixture of muon-following neutron events, and included an unknown NC cross-section scaling factor. After fixing all analysis procedures and parameters, the blindness constraints were removed. The analysis was then performed on the 'open' data set, statistically separating events into CC, NC, ES, and external-source neutrons using an extended maximum likelihood analysis based on the distributions of isotropy, cosine of the event direction relative to the vector from the Sun ($\cos\theta_\odot$), and radius within the detector. This analysis differs from the analysis of the pure D_2O data [2, 3, 12] since the spectral distributions of the ES and CC events are not constrained to the ^{8}B shape, but are extracted from the data. The extended maximum likelihood analysis yielded $1339.6^{+63.8}_{-61.5}$ CC, $170.3^{+23.9}_{-20.1}$ ES, $1344.2^{+69.8}_{-69.0}$ NC, and $84.5^{+34.5}_{-33.6}$ external-source neutron events. The systematic uncertainties on derived fluxes are shown in Table II. The isotropy, $\cos\theta_\odot$, and kinetic energy distributions for the selected events are shown in Fig. 2, with statistical uncertainties only. A complete spectral analysis including the treatment of differential systematic uncertainties will be presented in a future report. The volume-weighted radial distributions [$\rho = (R_{\rm fit}/600\ {\rm cm})^3$] are shown in Fig. 3.

The fitted numbers of events give the equivalent ^{8}B fluxes [14, 15] (in units of 10^6 cm^{-2}s^{-1}):

$$\phi^{\rm SNO}_{\rm CC} = 1.59^{+0.08}_{-0.07}({\rm stat})^{+0.06}_{-0.08}({\rm syst})$$
$$\phi^{\rm SNO}_{\rm ES} = 2.21^{+0.31}_{-0.26}({\rm stat}) \pm 0.10\ ({\rm syst})$$
$$\phi^{\rm SNO}_{\rm NC} = 5.21 \pm 0.27\ ({\rm stat}) \pm 0.38\ ({\rm syst})$$

and the ratio of the ^{8}B flux measured with the CC and NC reactions is

$$\frac{\phi^{\rm SNO}_{\rm CC}}{\phi^{\rm SNO}_{\rm NC}} = 0.306 \pm 0.026\ ({\rm stat}) \pm 0.024\ ({\rm syst}).$$

Adding the constraint of an undistorted ^{8}B energy spectrum to the analysis yields, for comparison with earlier results (in

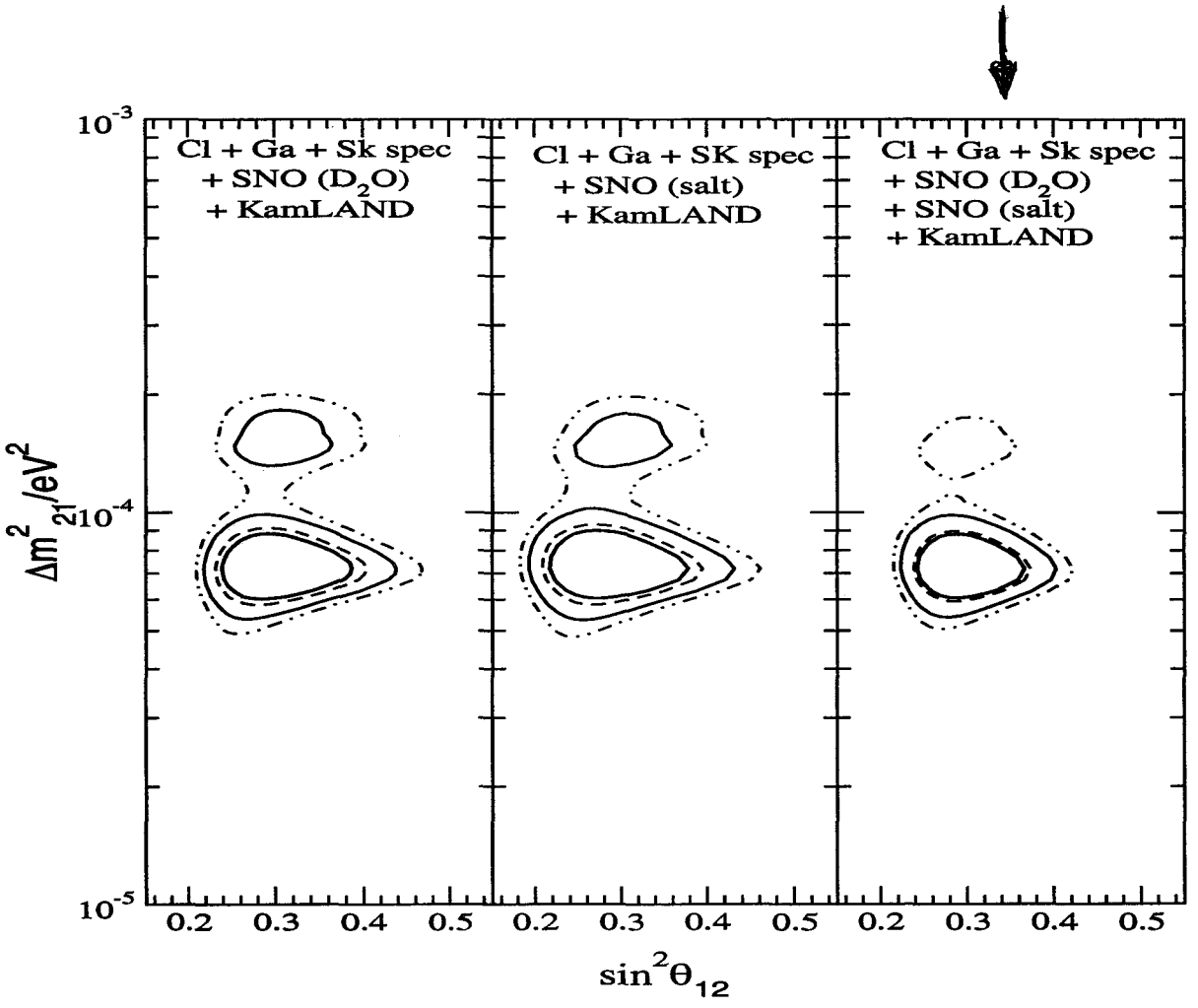

$$\Delta m^2_\odot \equiv \Delta m^2_{21} = 7.2 \times 10^{-5}\ \text{eV}^2\ ,$$

$$\sin^2\theta_\odot \equiv \sin^2\theta_{12} = 0.30\ ;$$

$$\cos 2\theta_{12} = 0.40; \quad \cos 2\theta_{12} > 0.20, \quad 99\%\ \text{C.L.}$$

- $\sin^2\theta_{12} = 0.50$ excluded at > 5 s.d.
- Low-LMA statistically favored
- High-LMA allowed only at $\sim 99.15\%$ C.L.

A. Bandyopadhyay et al, hep-ph/0309174

KamLAND 1 kTy

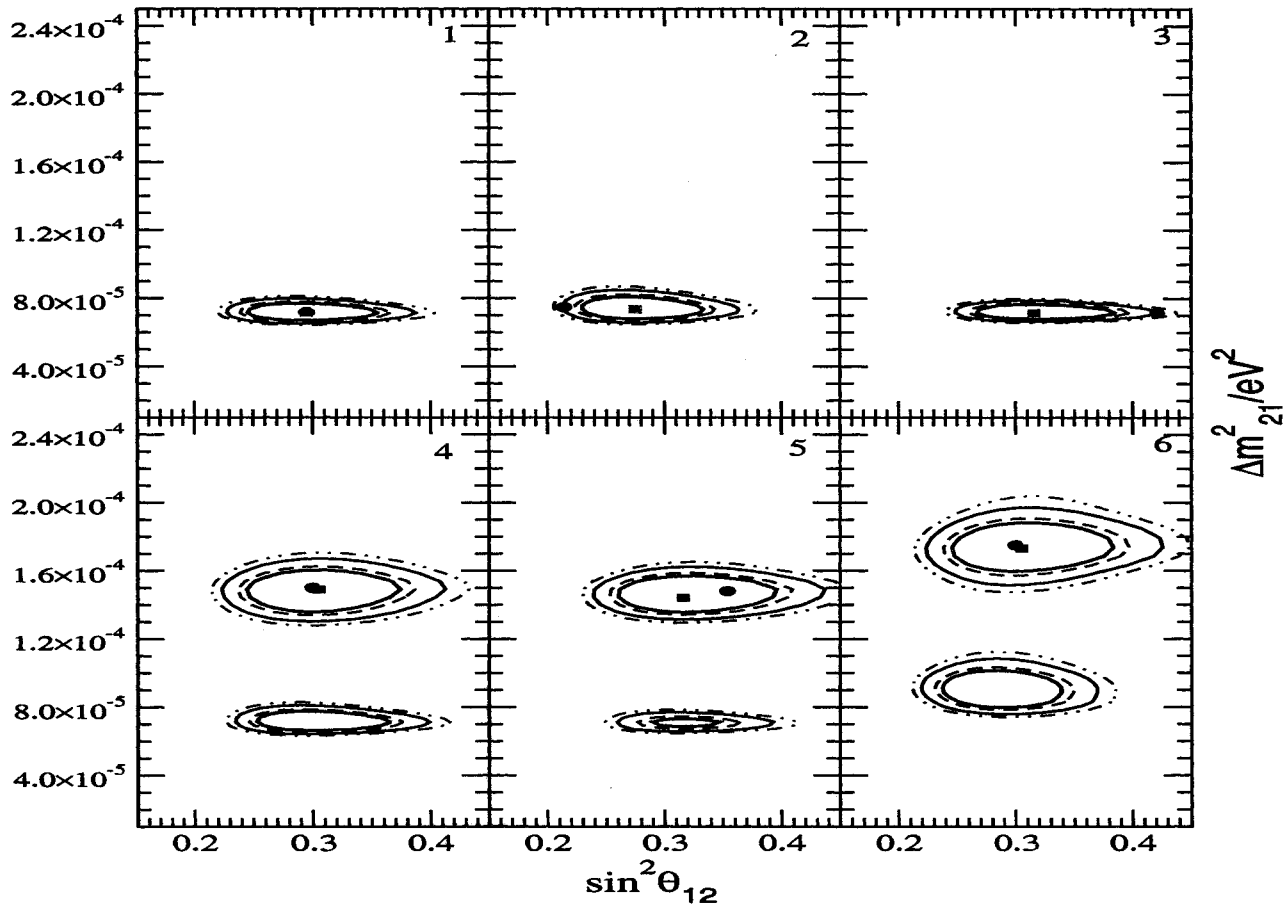

A. Bandyopadhyay et al, hep-ph/0309174

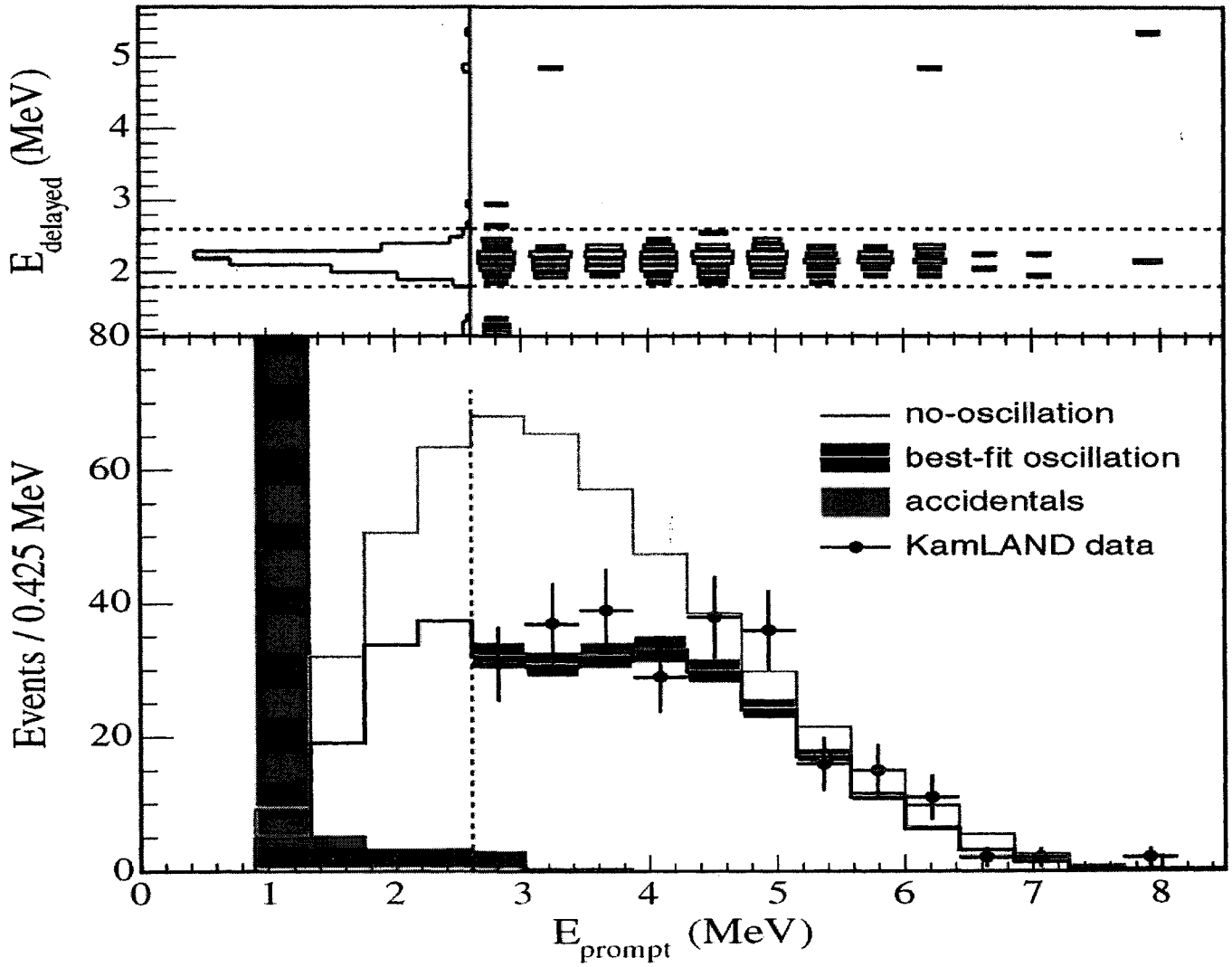

KamLAND: e^+−Spectrum Deformation

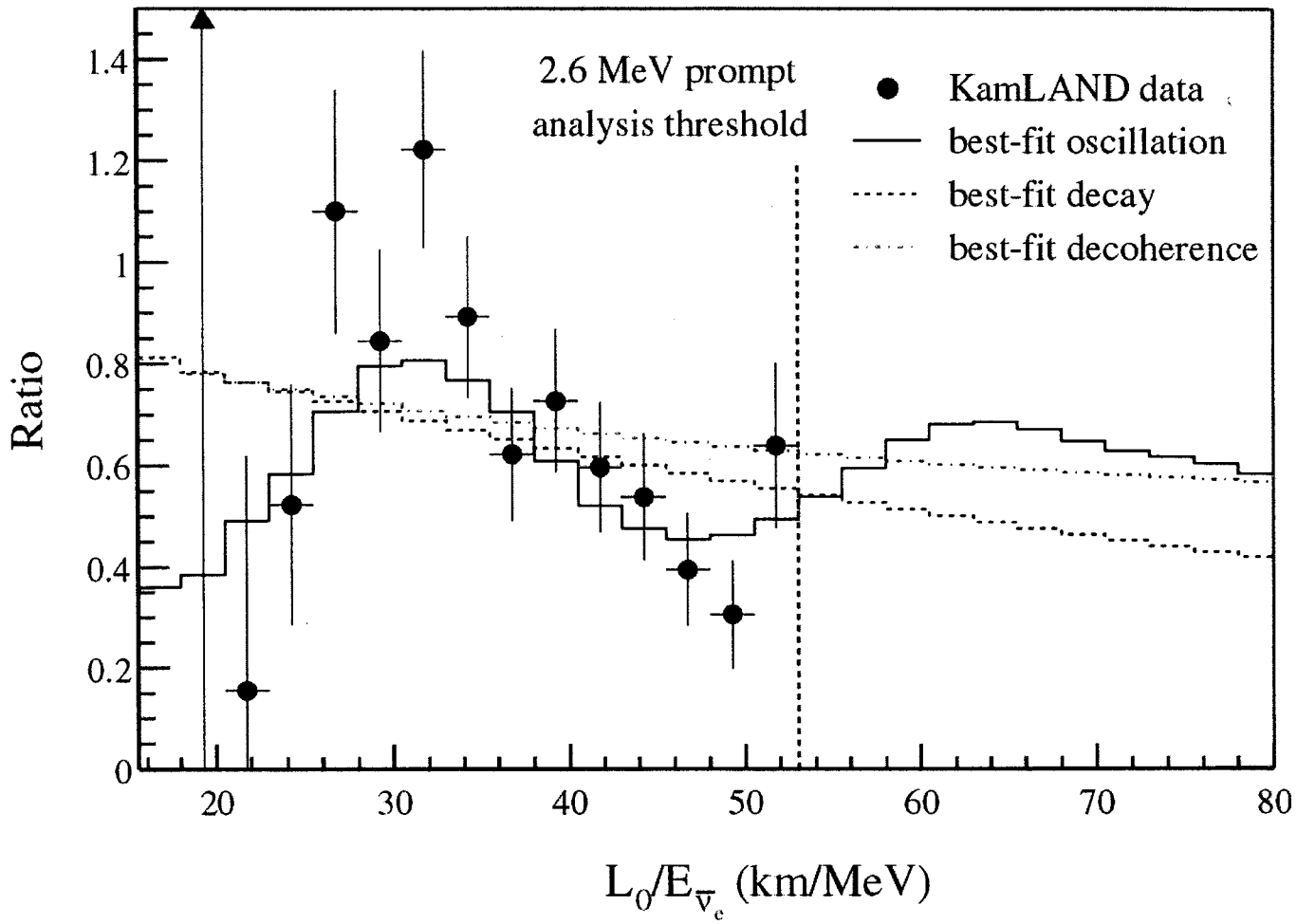

KamLAND: e^+−Spectrum Deformation

K2K: Spectrum Deformation

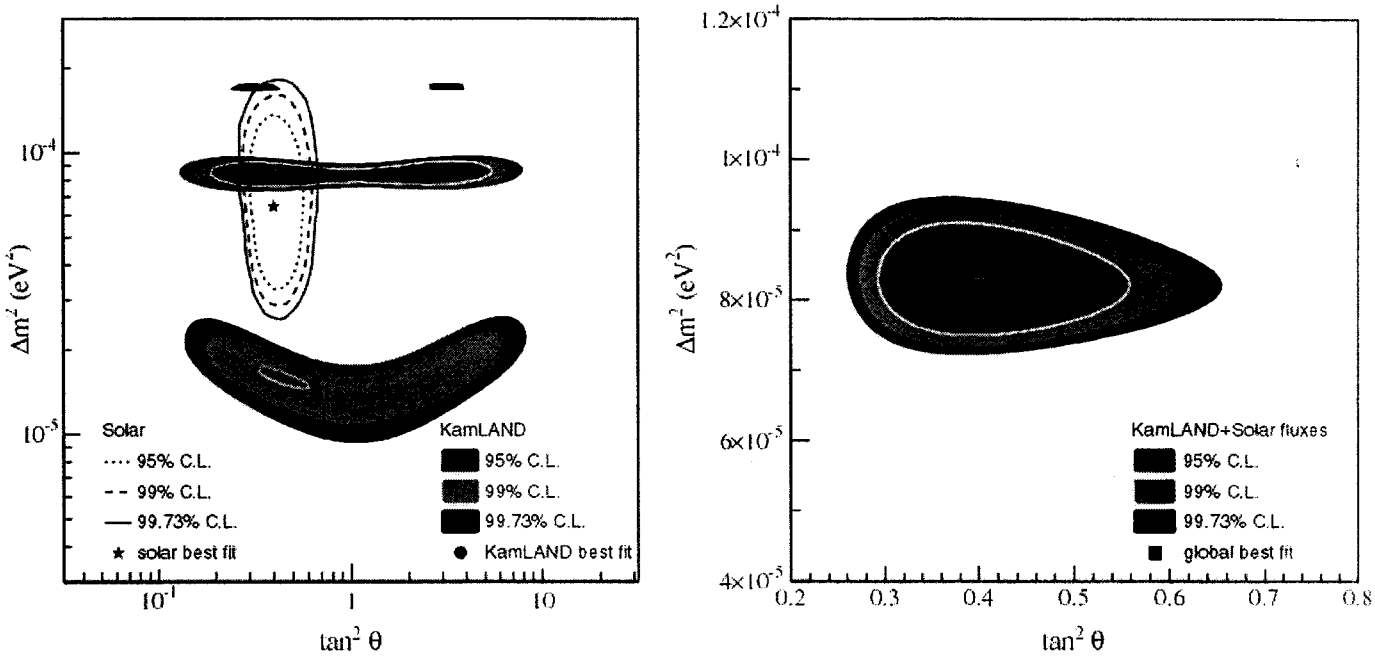

Impact of KamLAND Results on $\nu_\odot$ Oscillation Parameters

- High-LMA excluded at $> 3\sigma$

$$\Delta m^2_\odot \equiv \Delta m^2_{21} = (8.2^{+0.6}_{-0.5}) \times 10^{-5}\ \text{eV}^2\ ,$$

$$\tan^2\theta_\odot \equiv \tan^2\theta_{12} = (0.40^{+0.09}_{-0.07})\ ,$$

$$\cos 2\theta_{12} = 0.43; \quad \cos 2\theta_{12} > 0.21, \quad 99\%\ \text{C.L.}$$

J.N. BAHCALL, M.C. GONZALEZ GARCIA, C. PEÑA GARAY '0

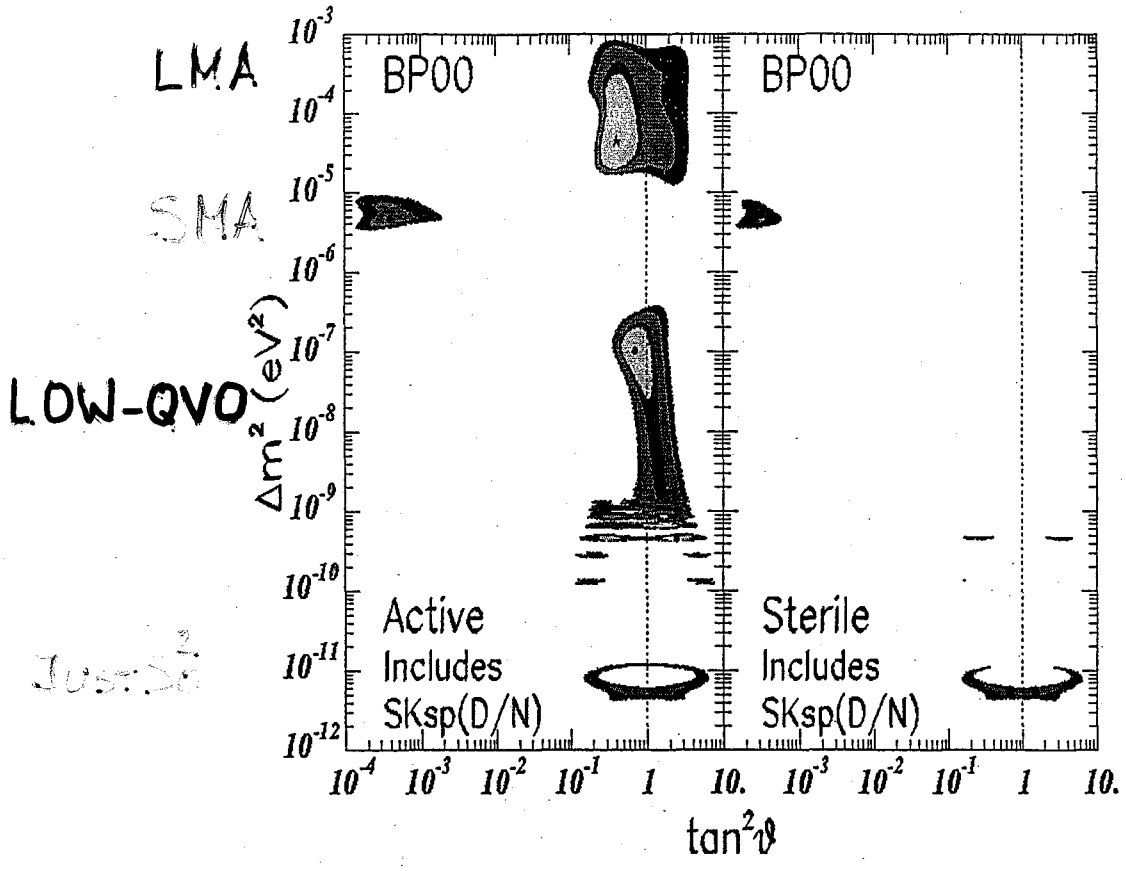

Figure 1: Global solutions including all available solar neutrino data. The input data include the total rates from the Chlorine [2], Gallium (averaged) [3, 5, 4], Super-Kamiokande [6], and SNO [1] experiments, as well as the recoil electron energy spectrum measured by Super-Kamiokande during the day and separately the energy spectrum measured at night. The C.L. contours shown in the figure are 90%, 95%, 99%, and 99.73% (3σ). The allowed regions are cutoff below $10^{-3}eV^2$ by the Chooz reactor measurements [22]. The local best-fit points are marked by dark circles. The theoretical errors for the BP2000 neutrino fluxes are included in the analysis.